Jana Steininger, BSc

Development of a Model Approach to describe the Kinetics of Voltage-gated Ion Channels in Non-excitable Cells

MASTER'S THESIS

to achieve the university degree of

Diplom-Ingenieurin

Master's degree programme: Biomedical Engineering

submitted to

Graz University of Technology

Supervisor

Univ.-Prof. Dipl.-Ing. Dr. techn. Christian Baumgartner

Institute of Health Care Engineering with European Testing Center of Medical Devices

Second Supervisor
Dipl.-Ing. Sonja Langthaler

Graz, February 2019

EIDESSTATTLICHE ERKLÄRUNG

AFFIDAVIT

Ich erkläre an Eides statt, dass ich die vorliegende Arbeit selbstständig verfasst, andere als die angegebenen Quellen/Hilfsmittel nicht benutzt, und die den benutzten Quellen wörtlich und inhaltlich entnommenen Stellen als solche kenntlich gemacht habe. Das in TUGRAZonline hochgeladene Textdokument ist mit der vorliegenden Masterarbeit/Diplomarbeit/Dissertation identisch.

I declare that I have authored this thesis independently, that I have not used other than the declared sources/resources, and that I have explicitly indicated all material, which has been quoted either literally or by content from the sources used. The text document uploaded to TUGRAZonline is identical to the present Master's thesis/diploma thesis/doctoral dissertation.

Datum / Date	Unterschrift / Signature

Die Technische Universität Graz übernimmt mit der Betreuung und Bewertung einer Masterarbeit keine Haftung für die erarbeiteten Ergebnisse: Eine positive Bewertung und Anerkennung (Approbation) einer Arbeit bescheinigt nicht notwendigerweise die vollständige Richtigkeit der Ergebnisse.

Acknowledgements

After an intensive period of almost a year today is the day: writing these lines is the finishing touch on my Master's thesis. It is now time to thank all the people that have made the completion of this thesis possible. Without their help and support, I would not be able writing these lines right now. Some persons deserve particular appreciation for their contributions.

First, I would like to express my gratitude to my supervisors, Univ.-Prof. Dipl.-Ing. Dr. techn. Christian Baumgartner and Dipl.-Ing. Sonja Langthaler. Their patient guidance, support and expert advice have been invaluable throughout all stages during the act of creation of this thesis.

I would also like to thank my friends and colleagues for their helpful advices and support, the sincere friendship and for always being there for me. They have made the last seven years to a period of my life I will always look back on with pleasure.

Last but not least, I want to thank my family and in particular my parents at that point for their unfailing mental and financial support and their continuous encouragement throughout my life and especially my years of study. I never had to worry about anything existential and could, actually can always rely on being supported unconditionally at any time. This accomplishment would not have been possible without them.

Thank you.

Entwicklung eines Modellansatzes zur Beschreibung der Kinetik von spannungsgesteuerten Ionenkanälen in nicht-erregbaren Zellen

Zusammenfassung

Ionenkanäle können zum malignen und metastasierenden Verhalten von Krebszellen beitragen, weshalb deren Modulation ein vielversprechendes Ziel der Onkologie darstellt. Die Krebsforschung fokussiert sich deshalb zunehmend auf die Beschreibung des Verhaltens von Ionenkanälen in Krebszellen unter verschiedenen Bedingungen. Der Fokus dieser Arbeit liegt auf der Simulation der Kinetik von Ionenkanälen in einer Lungenkrebszelllinie. Das Modell beinhaltet fünf Kanäle, die in A549 Zellen exprimiert sind und modelliert Strom-Spannungskurven sowohl von den einzelnen Ionenströmen, als auch vom Gesamtstrom. Durch das Variieren der Kanalanzahl im Modell kann die Blockade einzelner Kanäle simuliert werden. Das Modell belegt basierend auf der Implementierung der Kanäle $K_V1.3$, $K_{Ca}1.1$, $K_{Ca}3.1$, $K_{2P}3.1$ und CRAC (ORAI1), dass $K_V1.3$ Kanäle bezüglich ihrer Anzahl die größte Gruppe der fünf Kanäle sind.

Schlüsselwörter: A549 – Ionenkanäle – Modell – Lungenkrebs – nicht-erregbar

Development of a Model Approach to describe the Kinetics of Voltage-gated Ion Channels in Non-excitable Cells

Abstract

Ion channels can participate to the malignant and metastatic behaviour of cancer cells. Therefore, modulating those channels proves to be a promising approach in cancer therapeutics. For that reason, research increasingly focuses on the behavior of ion channels in cancer cells under various conditions. The present thesis targets at the simulation of the kinetics of ion channels in a lung cancer cell line. The developed model includes five ion channels that are expressed in A549 cells and provides current-voltage-curves of the individual ion currents as well as of the total ionic current. By adapting the number of channels, the blockage of specific channels can be simulated. Results show that $K_V1.3$ channels make up the largest group among all channels considered in the model, when implementing $K_V1.3$, $K_{Ca}1.1$, $K_{Ca}3.1$, $K_{2P}3.1$ and CRAC (ORAI1).

Keywords: A549 – ion channels – model – lung cancer – non-excitable

Table of Contents

List of Abbreviations

2P	Two-pore
ASIC	Acid-sensitive ion channel
BK	Big conductance potassium channel
Ca	Calcium
cAMP	Cyclic adenosine monophosphate
cDNA	Complementary deoxyribonucleic acid
Cl	Chloride
CLT	Clotrimazole
CNG	Cyclic nucleotide gated channel
CRAC	Calcium release-activated calcium channel
DNA	Deoxyribonucleic acid
ENaC	Epithelial sodium channel
GIRK	G-protein inwardly rectifying potassium channel
HCN	Hyperpolarization activated cyclic nucleotide gated channel
hIK	Human intermediate conductance potassium channel
I	Current
I_{inst}	Instantaneously activating current
I_{td}	Time-dependent activating current
IK	Intermediate conductance potassium channel
ir	Inwardly-rectifying
K	Potassium
KChIP	Voltage-gated potassium channel interacting protein
MgTX	Margatoxin
minK	Minimal potassium channel subunit
mRNA	Messenger ribonucleic acid
Na	Sodium
NSCLC	Non-small cell lung cancer
PCR	Polymerase chain reaction
pH	Potential hydrogen
RNAi	Ribonucleic acid interference

RT-PCR	Reverse transcription polymerase chain reaction
SCLC	Small cell lung cancer
shRNA	Short hairpin ribonucleic acid
siRNA	Small interfering ribonucleic acid
SK	Small conductance potassium channel
SOC	Store-operated calcium channel
SOCE	Store-operated calcium entry
STIM	Stromal interaction molecule
TEA	Tetraethylammonium
TPC	Two pore channel
TRP	Transient receptor potential channel
TRPA	Transient receptor potential ankyrin channel
TRPC	Transient receptor potential canonical channel
TRPM	Transient receptor potential melastatin channel
TRPML	Transient receptor potential mucolipin channel
TRPN	Transient receptor potential no mechanoreceptor potential channel
TRPP	Transient receptor potential polycystin channel
TRPV	Transient receptor potential vanilloid channel
TTX	Tetrodotoxin
V	Voltage

List of Symbols

$[x]_i$	Intracellular concentration of an ion x
$[x]_o$	Extracellular concentration of an ion x
C_m	Membrane capacitance
$C_{specific}$	Specific membrane capacitance
E_{rev}	Reversal potential
E_x	Equilibrium potential of an ion x
F	Faraday constant
g_x	Membrane conductance of an ion x
h	Gating variable for sodium inactivation
I_{ion}	Total ionic current
I_m	Total membrane current
I_x	Current of an ion channel x
m	Gating variable for sodium activation
n	Gating variable for potassium activation
N_x	Number of channels of an ion x
$p_i(V)$	Probability of a gate being in open state
$p_{i\infty}(V)$	Steady-state value
P_x	Permeability of an ion x
Q_{10}	Temperature coefficient
R	Universal gas constant
r	Radius
t	Time index
T	Temperature
V_m	Membrane potential
z_x	Oxidation state of an ion x
$\alpha_i(V)$	Opening rate constant
$\beta_i(V)$	Closing rate constant
$\tau_i(V)$	Time constant

List of Tables

List of Figures

1. Introduction

1.1. Principles of cellular electrophysiology

Typically, cells are enveloped by a phospholipid bilayer, the plasma membrane. Generally, physiological processes depend on the flux of ions across the plasma membrane of a cell, which acts as a selective barrier. The ionic concentration difference between intra- and extracellular space results in concentration gradients that cause the diffusion of particles from higher to lower concentration, which in term releases energy (Gibbs energy). Assuming that the membrane is selectively permeable for potassium ions, the movement of positively charged potassium ions out of the cell will render the cell negatively charged. This will start to attract the positively charged potassium ions to return back into the cell, caused by electrical energy. [1]

The diffusion of potassium ions continues until the two forces are in equilibrium and there is no further net movement at a certain voltage. This condition is called equilibrium potential or Nernst potential [1]:

$$E_x = \frac{RT}{z_x F} ln \frac{[x]_o}{[x]_i} \quad (1)$$

where E_x is the equilibrium potential of an ion x, R is the universal gas constant, T the temperature in Kelvin, z_x the oxidation state of an ion x, F the Faraday constant and $[x]_i$ and $[x]_o$ the intra- and extracellular concentration of the ion x.

The membrane potential is known as the difference in electric potential between the intra- and extracellular space (always measured as the potential inside minus the potential outside) and occurs due to the relative permeability of the membrane to several ions, as well as to their distribution on either side of the membrane. If the membrane is only permeable for one ion species (which is very uncommon), the above-mentioned Nernst potential also describes the reversal potential. On the other hand, if the membrane is permeable for several ion species, the membrane potential at which no current flows can be described with the Goldman-Hodgkin-Katz equation, which considers the presence of potassium (K), sodium (Na) and chloride (Cl) ions [2]:

$$E_{rev} = \frac{RT}{F} log \frac{P_K \cdot [K]_o + P_{Na} \cdot [Na]_o + P_{Cl} \cdot [Cl]_i}{P_K \cdot [K]_i + P_{Na} \cdot [Na]_i + P_{Cl} \cdot [Cl]_o} \quad (2)$$

where E_{rev} is the reversal potential described as a weighted mean of all Nernst potentials and P_x is the permeability of the respective ion x.

In a current-voltage plot, the reversal potential is the point where the current is zero, which is, figuratively seen, the intersection of the graph with the x-axis. At this point, there is no current flow and the ion flux reverses its direction, what is the reason why it is called reversal potential. [3]

The process of the membrane potential getting less negative is called depolarization, whereas hyperpolarization describes the process of the membrane potential becoming more negative. In excitable cells, like neurons or muscle fibers, changes in the membrane potential generate an action potential if the depolarization exceeds a certain threshold value. [4]

The potential of an unstimulated cell is known as resting potential. In most excitable cells mainly potassium channels are responsible for maintaining the resting membrane potential. Therefore, the resting potential moves mostly in a range near the equilibrium potential of potassium ions. [5]

For generating action potentials, or in general, for changing the membrane potential, it is necessary that ions flow across the membrane. Specialized proteins facilitate this flux of ions across the membrane. One category of these proteins make up the ion channels. [1]

1.2. Ion channels

The cell membrane serves as a selective barrier between intra- and extracellular space. It is a phospholipid bilayer that acts as an electrical insulator. On the one hand, it is permeable to small uncharged, polar molecules, lipophilic ones, gases and water, whereas on the other hand, it is impermeable to ions, large uncharged polar molecules, macromolecules and charged polar molecules. [5]

Ion channels are integral membrane spanning proteins that allow the passive flow of ions across the cell membrane in the direction of an electrochemical gradient. They are effective in controlling the membrane permeability to small water-soluble particles. In order to reach this effectiveness, ion channels have special properties. They form an aqueous pore that connects the intracellular- with the extracellular medium and show a selective permeability.

Additionally, they have a gating mechanism, which is a change in protein conformation and switches between closed and open conformational states. [1]

According to their gating mechanism, ion channels are classified into three subgroups [1]:

- Voltage-gated ion channels that open or close depending on the membrane potential
- Ligand-gated ion channels that open or close depending on the binding of an extracellular factor, like a hormone or neurotransmitter
- Second messenger operated channels that open or close in response to an intracellular factor, like calcium ions or activated G protein subunits

Additionally, the gating can be controlled by several other factors like temperature changes and mechanical forces (e.g. pressure or membrane stretch) [3, 5].

According to Ohm's law, the current through an ion channel is described as the membrane conductance times the electrochemical driving force [3]:

$$I_x = g_x \cdot (V_m - E_x) \tag{3}$$

where I_x is the net ion current per unit of membrane surface area, g_x is the membrane conductance and the term V_m-E_x is the membrane potential minus the equilibrium potential of an ion x, constituting the electrochemical driving force.

1.2.1. Voltage-gated ion channel superfamily

Voltage-gated ion channels are integral membrane proteins that open and close in response to membrane potential changes. They are part of the voltage-gated ion channel superfamily and can be classified according to the ions the channels are permeable for. [6]

The International Union of Pharmacology has developed a naming system for ion channels that are part of the voltage-gated ion channel superfamily. This system describes all ion channels based on their functional characteristics and structural relationships. The name of the ion channel starts with the principal permeating ion, like for example K for potassium. Often written as subscript, the principle regulator or classifier of the channel follows, like e.g. "V" for voltage, or "Ca" for calcium. Another structural classification make up the potassium channel families K_{ir} and K_{2P}, where "ir" stands for inwardly-rectifying and "2P" denotes for two-pore. Following the subscript, a number describes the gene family and, separated by a dot, a second number describes the specific channel isoform. Channel families without a principal permeating ion, can be named according to their gating regulator or classifier, like

e.g. “CNG” for cyclic nucleotide gated channel family, “HCN” for hyperpolarization activated cyclic nucleotide gated channel family, “TRP” for transient receptor potential channel family and “TPC” for two pore channel family. [7]

Figure 1 shows an overview of the voltage-gated ion channel superfamily and the structures of the various ion channel groups. The figure is adapted from Yu et al. [6].

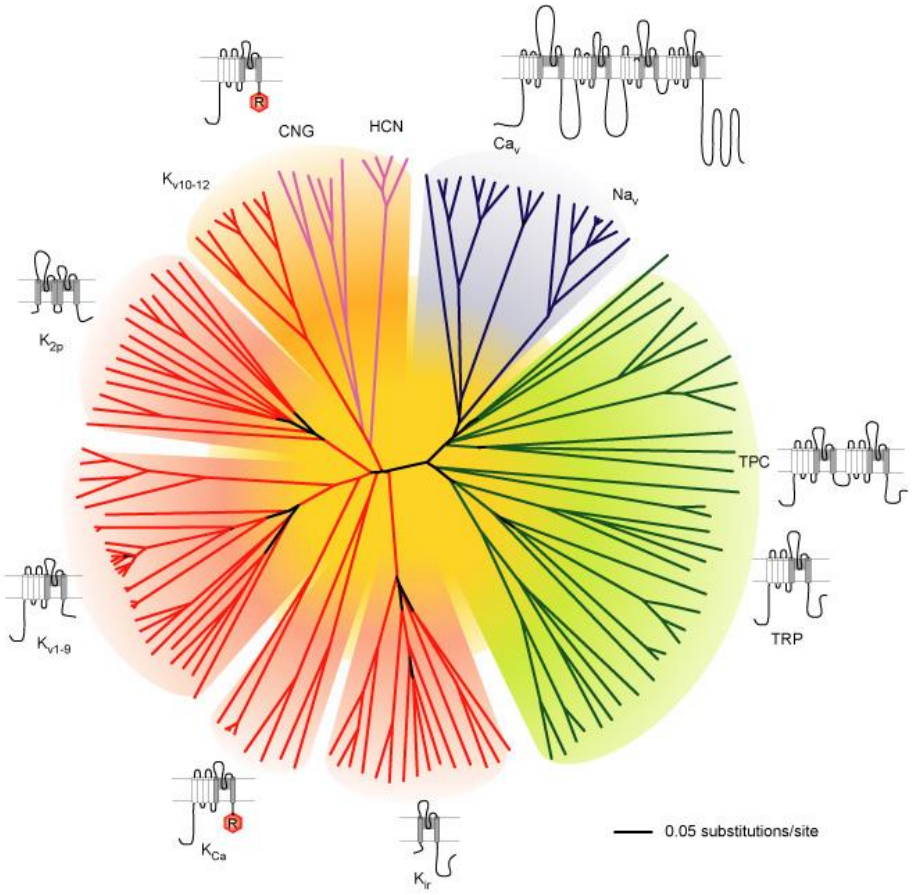

FIGURE 1: The voltage-gated ion channel superfamily (cf. [6])

In general, ion channels are composed of one or more protein subunits. The subunit that forms the pore of the channel is called principal subunit. If an ion channel has more than one principal subunit it is called multimer. Furthermore, if the subunits are identical, they are called homomers. In case they are not identical, they are called heteromers. In addition to the principal subunit, ion channels may also have auxiliary subunits, which can modulate the function of the principal subunit. [7]

Depending on their structure, channels of the voltage-gated ion channel superfamily can be divided into four architectural subgroups [6].

The first of four subgroups is characterized by four homologous domains that make up the

principal α-subunit. Every domain contains six transmembrane α-helices, referred to as S1-S6. S5 and S6 in combination with a membrane-reentrant loop in between, form the pore and the selectivity filter, whereas the segment S4 acts as voltage sensor for the channel. Voltage-gated sodium channels, as well as voltage gated calcium channels, which have a very similar structure, count among this subgroup. [6]

Voltage-gated potassium channels are part of the second subgroup. They are composed of tetramers of α-subunits, each consisting of six transmembrane proteins as well, resembling one of the four homologous domains of the first subgroup. Calcium-activated potassium channels, CNG channels, HCN channels, together with TRP channels, also belong to this subgroup, as they have the same architecture. [6]

The third and most basic subgroup regarding the architecture make up the inwardly rectifying potassium channels. They consist of four subunits, each having two transmembrane segments M1 and M2, which are equal in function and structure to the S5 and S6 segment of the voltage-gated sodium, calcium and potassium channels. The two-pore motif potassium channels characterize the fourth subgroup. As suggested by the name, they consist of two of the previously mentioned pore motifs of the third subgroup. [6]

Besides the mentioned pore-forming alpha-subunits, some channels have accessory subunits that have very diverse functions like e.g. modulation of the conductance of the channel or affection of the gating properties [5]. Voltage-gated sodium channels have four known auxiliary subunits called $Na_V\beta1$ to $Na_V\beta4$ that interact with the α-subunits and regulate their subcellular localization and physiological properties. Voltage-gated calcium channels also have up to four auxiliary subunits ($Ca_V\alpha2$, $Ca_V\beta$, $Ca_V\gamma$, $Ca_V\delta$) which regulate cell surface expression and modulate gating properties. Since the structure of the α-subunits of voltage-gated potassium channels is different, they also have diverse auxiliary subunits. Three $K_V\beta$ subunits ($K_V\beta1$-3) are often associated with K_V1 channels, whereas K_V4 channels interact with the four K_V-channel interacting proteins (KChIP) KChIP1-4 that modify the functional properties of the channels. K_V7, K_V10 and K_V11 channels are associated with five auxiliary subunits that are called minK-like, regulating the channel function. Moreover, novel studies suggest that K_V3 and K_V4, and maybe even all K_V-channels, associate with minimal potassium (minK)-like subunits. There are four known $K_{Ca}\beta$-subunits, one of them associated with the $K_{Ca}1$, 4 and 5 families. Their impact on the channel function is still subject of research. [6]

For the opening and closing of voltage-gated ion channels, energy, derived from changes of

the membrane potential, is necessary. The membrane potential changes result in a cascade of conformational changes, which in turn opens the ion channel. First, the energy is transmitted to the S4 segment (the voltage sensor) of the channel, resulting in a movement of this segment, which in turn moves the segments S5 and S6 that finally open or close the pore. While the S4 segment moves with the same speed in all kind of channels, the movement of the S5 and S6 segment happens at a different speed. Accordingly, the fact that Na_V-channels open faster than K_V-channels results from the movement of the S5 and S6 segment at different speed. A channel, opened by depolarization can be closed again by repolarization of the membrane. Despite ongoing depolarization, some channels (like Na_V-channels) do not stay in the open position after activation, but they close again, which is called inactivation. For this process, the inactivation domain enters the pore, binds to a receptor and thus blocks the channel. In order to reverse the inactivation, the membrane has to be repolarized. Subsequently, the channel can be opened again, a process called reopening. [5]

Since several different voltage-gated ion channels act simultaneously, they may affect each other. As an example, the interaction between voltage-gated sodium, calcium and potassium channels can be considered. When the voltage-gated sodium channels open, sodium leaks into the cell, causing a depolarization of the membrane potential. The depolarization induces the opening of the voltage-gated calcium channels, which in turn causes an influx of calcium. Both, the influx of calcium and sodium into the cell causes an opening of the voltage-gated potassium channels allowing the outflow of potassium ions and thus, the repolarization of the membrane and closing of the voltage-gated sodium and calcium channels. [8]

1.2.2. Ion channels and cancer cells

Cancer emerges from an uncontrolled, enhanced proliferation, aberrant differentiation or impaired apoptosis of cells. It can be caused by many environmental factors, but it has been shown, that several ion channels contribute to the emergence of cancer as well. [1, 9]

Cells can be classified into excitable and non-excitable cells, which differ from each other in their ability to generate action potentials. In non-excitable cells, like cancer cells and other proliferating cells, which do not have the ability to generate action potentials, it has been displayed that membrane potential changes control several critical cellular functions like proliferation, migration and differentiation. In addition, it seems that depolarization itself

may be enough to cause neoplastic transformation. Since ion channels contribute to the changes in the membrane potential, it is obvious that ion channels are also present in non-excitable cells, where they regulate multiple pathophysiological functions that participate to its tumorous behavior. Generally, the membrane potential of cancer cells tends to be more depolarized (in the range of -5 to -55 mV), having a lower absolute value, than its healthy counterparts. [1, 10, 4]

Both, in individual non-excitable as well as in individual excitable cells, the membrane potential changes during the cell cycle progression. A cell cycle is divided into 5 phases. It starts with the G0 phase, which implicates non-proliferating cells. Next in the G1 phase, the cells get primed for the DNA replication. After this, the S phase follows, where the DNA replication happens, leading to the G2 phase, where the cells are getting ready for mitosis. Finally, there is the M phase or mitosis, where the cells are completely divided into two separated cells. The fluctuation of the membrane potential during the cell cycle depends on the expression of various ion channels and is a very complex process. During the cell cycle of cancer cells, several voltage-gated ion channels interact with each other and thus contribute to the changes in the cell cycle. The opening of voltage-gated Na^+ and/or Ca^{2+} channels causes a depolarization of the membrane, since positive ions move into the cell, which seems to be essential for the transition from the G0/G1 phase to the S phase of the cancer cell cycle. During the S phase the closing of Na^+ and/or Ca^{2+} channels and the opening of K^+ channels respectively, induces a hyperpolarization of the cell membrane. Mitosis is related to a more depolarized membrane potential, which is caused by an increased concentration of intracellular Na^+ and/or Ca^{2+}. The depolarization and an enhanced Ca^{2+} entry allows an activation of Ca^{2+}-activated K^+ channels and Cl^- channels, which generates an outward flux of Cl^- and K^+, that is in turn responsible for the cell shrinkage before cell division, since water leaves the cytoplasm. Using special channel blockers can cause a cell cycle arrest and therefore a reduced propagation of cancer cells. [10, 11]

Since ion channels obviously play an important role in cancer pathology, they recently have become an important target for the treatment of cancer and cancer research. More precisely, ongoing research shows that aberrant expression of specific ion channels is related to various stages of cancer and malignant transformation. Furthermore, the manipulation of the channel's activity provides an approach for cancer treatment. The most common attempts of cancer treatment via ion channels are ion channel-inhibiting drugs. A big

problem of using these so-called blockers is that they may target also channels expressed in healthy tissues. An example for this are K_V11.1-blockers. While blocking these channels in tumor tissue results among others in reducing proliferation in tumor cell lines, the blockage in healthy tissue can slow down cardiac repolarization and may result in a life-threatening ventricular arrhythmia. To overcome this problem another approach is to target the channels in a specific functional state, which is predominant in cancer cells. If for example the K_V11.1 blockers target the channels in open state, they may have a positive effect on the treatment of tumor cells, while leaving the cardiac channels unaffected, since they are mainly in a deactivated or inactivated state. [10, 11]

1.3. Ion current models

There exist many models covering the membrane potential of cells, but most of them describe the behavior of excitable cells. Since non-excitable cells are similar to excitable cells regarding ionic concentration, certain components of existing models for excitable cells can be used to generate a model for the description of non-excitable cells. The first model to describe the behavior of excitable cells was developed in 1952 by Hodgkin and Huxley. They presented an electronic circuit to model the transmembrane potential and the ionic currents of a giant squid axon. Furthermore, they described how the membrane potential changes over time and thus, they modelled initiation and propagation of action potentials of the giant squid axon. Although the model was developed for a specific type of excitable cells years ago, it is still the basis of many of the recently developed ion channel models. [12]

In the original Hodgkin-Huxley model, the cell membrane is represented by a capacitor and the membrane potential is indicated as potential from the inside of the cell minus the one from the outside of the cell. Conductances represent the permeability of the voltage-gated ion channels, batteries represent the electrochemical driving force generated by each ion species, whereas the externally applied current is indicated as a current source. Hodgkin and Huxley divided the ionic current crossing the membrane of the giant squid axon into three components, two of them carried by sodium and potassium and the third component, described as leakage current, is carried by chloride and other ions. So-called gates describe the dynamics of the ion channels in their model. Each gate is controlled by gating particles, which can be either in closed or in open position. The movement between open and closed

position is controlled by changes in the membrane potential. [13, 7]

The Hodgkin-Huxley model reproduces the biophysical properties of an action potential of the squid giant axon. Hodgkin and Huxley described the behavior of the cell as an electronic circuit by the following equation [13]:

$$I_m = C_m \frac{dV_m}{dt} + I_{ion} \tag{4}$$

where C_m represents the membrane capacitance, V_m the membrane potential, t the time index, I_{ion} the ionic current across the membrane and I_m the total membrane current. As previously mentioned, the total ionic current across the membrane of the squid giant axon is the sum of the three individual ion currents and described as follows [13]:

$$I_{ion} = g_{Na}(V_m - E_{Na}) + g_K(V_m - E_K) + \bar{g}_L(V_m - E_L) \tag{5}$$

where g_x is the ionic conductance and E_x is the equilibrium potential of the ion x. The conductances g_{Na} and g_K are suggested to be time- and voltage-dependent, whereas the leakage conductance is considered constant. The ionic conductance is described as the product of individual gate probabilities times the maximum conductance of the membrane to a specific ion, which in turn is defined as the single channel conductance times the number of channels. The gate probabilities are described by the two rate constants $\alpha_i(V)$ (for the transition from non-permissive to permissive, open state) and $\beta_i(V)$ (for the transition from permissive to non-permissive, closed state of a gate), both dependent on the membrane potential. The gate probabilities are described by the following relationship [14]:

$$\frac{dp_i}{dt} = \alpha_i(V)(1 - p_i) - \beta_i(V)p_i \tag{6}$$

where p_i describes the probability of an individual gate being in the permissive, open state. From this relationship, the steady-state value, where opening and closing rates are equal, and the time constant $\tau_i(V)$ that describes the time course for approaching the steady-state value, can be derived and described as follows [14]:

$$p_{i,t\to\infty} = \frac{\alpha_i(V)}{\alpha_i(V) + \beta_i(V)} \tag{7}$$

$$\tau_i(V) = \frac{1}{\alpha_i(V) + \beta_i(V)} \tag{8}$$

Using equation (7) and (8) and plugging it in equation (6), the time dependence of the gate

probabilities can also be described by:

$$\frac{dp_i}{dt} = \frac{p_{i,\infty} - p_i}{\tau_i} \tag{9}$$

With these general relationships and introducing the gating variables “m” for sodium activation, “h” for sodium inactivation and “n” for potassium activation, Hodgkin and Huxley described the ionic current across the membrane as [14]:

$$I_{ion} = \bar{g}_{Na} m^3 h (V_m - E_{Na}) + \bar{g}_K n^4 (V_m - E_K) + \bar{g}_L (V_m - E_L) \tag{10}$$

The Hodgkin-Huxley approach can also be used to generate so-called multi-compartmental models. Whereas the classical Hodgkin-Huxley model only describes the behavior of the axon, multi-compartmental models describe the electrical responsiveness of an entire neuron. [7]

Another type of ion channel models are the so-called Markov models. While Hodgkin-Huxley-based models describe the probability of a channel being open as a product of gating variables, indicating that the gating particles act independently, Markov models describe the probability of the entire channel being in a number of possible states. This has the advantage that the data can be fitted more accurately, since there are more parameters available for fitting. Due to the higher accuracy, it is common to use Markov models to describe the behavior of a single channel. A disadvantage of Markov Models is, obviously, that there are more parameters available for fitting, which makes the simulation process much more complex and time-consuming than for Hodgkin-Huxley-based models. [7]

1.4. Patch Clamping

For a very basic form of measuring the membrane potential, called intracellular recording, principally two electrodes are required. If there is one electrode inside the cell and one electrode outside the cell, the potential difference between these electrodes can be measured as the membrane potential across the membrane. In the beginning of membrane potential measurements, cells like the giant squid axon with a diameter of 400-800 µm were measured with this technique using wire electrodes. [15]

The principle of voltage clamp was developed about the same time. It allows the direct measurement of the membrane current by keeping the membrane potential stable. With this technique, the user sets a holding potential in the beginning of the experiment. During

the experiment, the membrane potential is measured and compared to the given holding potential via a feedback amplifier. Any deviation of the recorded membrane potential from the previously set holding potential is corrected by current injection. The injected current then represents the ionic current over the membrane. [1]

In 1976, Neher and Sakmann used micropipettes with small tips with a diameter in small µm-range for pressing the tip of the electrode to the membrane of an isolated skeletal muscle fibre. With this technique they were able to electrically isolate a small patch of the membrane and thus, to monitor single channel ion currents. In 1980-1981, Neher and Sakman together with Sigworth, Marty and Hamill developed a high resistance seal between electrode and membrane, which is named “gigaseal”, due to the electrical resistance between the inside and the outside of the electrode being in the gigaohm-range. With this technique, the quality of recording improved. As a result, the technique makes it possible to record single channel currents or macroscopic currents, depending on further steps, since it reduces the noise level of the recording and it increases the current resolution. With this work, Neher and Sakmann received the Nobel Prize in Physiology and Medicine in 1991 and form the basis of the patch-clamp technique, as it is still used today. [1, 16, 15, 17, 18]

The patch-clamp technique has several configurations, which makes it very powerful and especially flexible, depending on the ion channels and the research interest. In principal, it can be classified into single channel and whole cell measurements, according to the number of ion channels to be measured. The most common patch-clamp configurations are [1]:

- Single-channel recording:
  - Cell-attached patch mode
  - Outside-out excised patch mode
  - Inside-out excised patch mode
- Macro-current recording:
  - Whole-cell mode
  - Perforated patch mode

Each of these configurations has advantages and disadvantages. Depending on the configuration, it is possible to manipulate the fluid either on the extracellular or on the intracellular side during the experiments. [1]

The main advantages of the patch-clamp technique are that it enables voltage-clamp because of the gigaseal formation, that there is a low background noise around the patch

and that it can be applied to a large variety of cells [15].

A major general drawback of the patch-clamp technique is that it requires lots of experience to obtain adequate results. Furthermore, the technique is very time-consuming which is why the automated patch-clamp technique was invented. Automated patch-clamp systems overcome the problem of complexity and required experience and additionally, they enhance the throughput of the conventional patch-clamp technique. There are two main categories to reach a high-throughput patch clamp system. The first method is the automation of the conventional patch-clamp technique and the second one is the development of an automated planar and lateral patch-clamp system. For the first one, conventional glass in combination with a fully automated patch clamp robot are used. Although this method already increases the throughput, it is not as high as it could be. That is why planar and lateral patch-clamping were invented and nowadays used in the majority of experiments. For this technique, a pore in a flat chip replaces the micropipette. As distinguished from the conventional patch-clamp technique, where the micropipette is brought to the cell, in this technique the cell to be investigated is positioned on the pore. Afterwards suction is applied to obtain a gigaseal whereon measurements in diverse configurations can be performed. Although this technique is an improvement regarding the throughput and the ability to adjust the pipette and the bath solution, the quality of the recordings is not as good as in conventional patch clamp. Furthermore, the costs are much higher, since the chip of the planar-patch clamp technique is a single-use tool. [19]

1.4.1. Methods for ion channel isolation

In order to model the behavior of ion channels of an ion species, or even of specific ion channels, and since single-channel patch clamp recordings are not always viable, it can be necessary to isolate the desired ion channel for the upcoming measurements. The following main methods to isolate ion currents are known [7, 17, 20]:

Hodgkin and Huxley used the ion substitution method for fitting the parameters of their model. They lowered the extracellular sodium concentration by replacing sodium ions in the standard extracellular solution with impermeant choline ions. Assuming that the independence principle holds and all ionic currents are independent, and thus, the other currents stay the same, they observed that the currents recorded with the two different extracellular solutions are different. This difference then can be used to conclude the sodium

current. The same approach can be used to manipulate the composition of the ionic solution to favor the movement of specific ions across the membrane. [7]

A very common approach to isolate currents is the channel isolation by blockers. Blockers are specific pharmacological compounds that, depending on the type, prevent certain types of currents flowing. Examples for established blockers are Tetrodotoxin (TTX), which blocks certain Na^+ channels, or Tetraethylammonium (TEA), which blocks certain K^+ channels. There exist also very selective blockers that block a specific ion channel. [7, 17]

From the molecular biological side, channels can be isolated by messenger ribonucleic acid (mRNA) transfection. For this method, complementary deoxyribonucleic acid (cDNA) or mRNA of a protein is expressed in a cell that normally do not express that protein, which is called heterologous expression. Heterologously expressed, ion channels can be studied in isolation from the original cell. Nowadays, the usage of small interfering RNA (siRNA) or short hairpin RNA (shRNA) is very common for the silencing or knock-down of proteins via RNA interference (RNAi). [7, 20]

Another approach for isolating specific ion currents is a kinetic one. As several ion channels activate and inactivate faster than others, ion currents can be isolated by studying a whole-cell recording at different time points, as long as the type of ion channels expressed in the cell and the approximate behavior of the channel are known. [17]

Since some subpopulations of several ion channels have voltage-dependent activation and inactivation currents, it is possible to isolate them from each other by voltage steps originating from different holding potentials. Depolarizing voltage steps applied from very negative holding potentials for example can activate transient A-type and delayed-rectifying potassium currents, whereas voltage steps from a more positive holding potential inactivates all transient A-type channels. Subtracting the currents of these two protocols effectively isolates the transient A-type potassium currents. [17]

2. Task

Ion channels play a fundamental role in almost all cellular processes like proliferation, differentiation and apoptosis. It has been shown that specific ion channels exhibit altered channel expressions, which can drive malignant and metastatic cell behavior in cancer cells. Thus, therapeutic strategies modulating ion channels prove to be promising in cancer therapeutics.

To be able to modulate ion channels in cancerous tissue, first it is important to understand the behavior and the kinetics of these channels. Since the expression and kinetics of ion channels in non-excitable cells are still persistent themes in research, a model will help to have a better understanding on how specific ion channels affect the tumorous behavior of a cell.

Based on existing ion current models and experimental data, a model approach should be developed to describe and simulate the kinetics of voltage-gated ion channels in non-excitable cells. In order to achieve a proper model, literature research on ion channel expression in cancer cells in general, on the human adenocarcinoma lung cancer cell line A549 and on ion channels expressed in this cell line has to be done. With the obtained results from literature research, a model approach should be derived to describe the kinetics of voltage-gated ion channels in A549 cells. The resulting model finally should be implemented in Matlab (Mathworks Inc., Natick, USA).

3. Material and Methods

3.1. Used Cell Line

The A549 cell line was established in the 1970ies through the removal and culturing of cancerous lung tissue of a 58-year-old Caucasian man. The cells are adenocarcinomic alveolar basal epithelial cells. In nature, the cells are squamous and responsible for the diffusion of particles across the alveoli of lungs. In vitro, A549 cells grow adherently as a monolayer, whereas in vivo they induce tumors in athymic mice. [21]

Generally, lung cancer is categorized into two types of cancer: Non-small cell lung cancers (NSCLC), which are again classified into three subgroups (squamous-cell carcinoma, adenocarcinoma and large-cell carcinoma) and small cell lung cancers (SCLC), according to the size and appearance of the malignant cells. Adenocarcinomas, like A549 cells, are the most common type of lung cancers and arise from small airway epithelial type II alveolar cells. This type of non-small cell lung cancer tends to grow not as fast as other types of lung cancer do and occurs in smoker's as well as in non-smoker's lungs, whereas squamous-cell and large-cell carcinomas strongly correlate with cigarette smoking. [22, 23]

For the further development and extension of the model, it is good to know the specific properties of A549 cells. According to Wang et al. [24], the specific membrane capacitance of A549 cells is 2.45 ± 0.57 µF cm^{-2}. Assuming the cells' form spherical, the actual membrane capacitance can be calculated with help of the general equation for spherical surfaces:

$$surface\ area = 4\pi r^2 \tag{11}$$

Literature reports 14.93 µm for the diameter of A549 cells measured by inverted microscopy [25]. Therefore, the actual membrane capacitance is:

$$C_m = C_{specific} \cdot surface\ area = 2.45 \frac{\mu F}{cm^2} \cdot 4\pi \cdot \left(\frac{14.93\ \mu m}{2}\right)^2 = 17.157\ pF$$

In addition, Liang et al. [26] report a resting cytosolic calcium concentration of about 295 nmol/L in A549 cells, which may be useful when implementing the calcium concentration into the model.

3.2. Ion channels expressed in cancer cells

The expression of ion channels in various cancer types is a very complex field of interest.

Many different ion channels are expressed in various cancer types, but it seems like there is no unifying pattern regarding a channel being over- or underexpressed. Another aspect that makes the relation between ion channel expression and cancer rather complex is that the mechanisms of the up- or downregulation of ion channels in tumor cells seems to be diverse. Divergent expression of ion channels in cancer cells regulates many cellular functions, with some of them contributing to various aspects of tumor progression. [10]

3.2.1. Potassium channels

According to their gating mechanism, potassium channels can be classified into five major subgroups [9]:

- Voltage-gated
- Ca^{2+}-activated
- Inwardly rectifying
- ATP-sensitive
- Background two-pore domain-containing

All of them belong to the voltage-gated ion channel superfamily and as its name implies, they are selectively permeable for K^+-ions.

The group of voltage-gated potassium channels consists of 12 subfamilies (K_V1-K_V12). Voltage-gated K^+-channels are activated by changes of the membrane potential. They essentially contribute to the maintenance of the resting membrane potential or the regulation of the membrane potential, respectively. In excitable as well as in non-excitable cells they cause an outward flow of potassium ions, which depolarizes the cell membrane. Since K^+ ions are the dominant cation in most of the cells, K^+ channels contribute to the regulation of the cell volume, as the cations flow out of the cell through K^+ channels. [9, 11, 8]

According to the single channel conductance, the group of calcium-activated potassium channels can be further divided into three subgroups: big (BK), intermediate (IK) and small (SK). The activation of the IK channel, also known as $K_{Ca}3.1$, and the activation of the SK channels ($K_{Ca}2.1$-3) is only Ca^{2+} dependent, whereas the BK channel, also known as $K_{Ca}1.1$, can be activated via calcium ions and membrane potential changes. [27, 28]

Several different K^+-channels have been identified in a range of cancers, in accordance with the paradigm that an enhanced efflux of K^+-ions is associated with apoptosis. Vice versa, a

decreased K^+-efflux enhances apoptosis. Furthermore, voltage-gated potassium channels are involved in cell proliferation and in the control of the cell cycle. One of the cancer related potassium channels is the voltage-gated delayed rectifier $K_V11.1$ channel (also called hERG1 channel) which contributes to the tumorous cell proliferation and survival. It is upregulated e.g. in acute myeloid leukemia cells and esophageal, endometrial, gastric and colon tumors, as well as in gliomas and Non-Hodgkin lymphomas. An inhibition of the $K_V11.1$ channel causes a reduced proliferation of cancer cell lines and as well apoptosis. In addition, the voltage-sensitive ether à-go-go potassium channel $K_V10.1$ (also called EAG1) is often mentioned in the context with cancer cell proliferation. Usually, the channel expression is limited to the brain, but aberrant expression of the $K_V10.1$ channel has been reported in various cancer cell lines and tumor types. Examples are e.g. breast, colon, esophageal and gastric cancer, as well as gliomas and melanomas. Interestingly, the voltage-gated $K_V1.5$ channel is downregulated in gliomas, breast and lung cancer, respectively. In addition, the $K_V1.3$ channel is often associated with cancer. It is upregulated in tumorous breast biopsies, colon cancer cells and lymphomas, whereas it seems to be downregulated in metastatic prostate tumors and cell lines. Furthermore, the $K_V1.3$ channel seems to be expressed in colorectal cancer and lung adenocarcinomas and it is known to operate in conjunction with $K_{Ca}3.1$, which is a Ca^{2+}-activated potassium channel. [10, 9, 29, 30, 11, 31, 32]

Moreover, not only voltage-gated K^+-channel, but also several two-pore, inwardly rectifying and Ca^{2+}-activated potassium channels are related to cancer. As an example, the inwardly rectifying $K_{ir}3.1$ channel is overexpressed in breast and pancreatic tumors, whereas the two-pore acid-sensitive $K_{2P}9.1$ channel is upregulated in colon and breast tumors and the two-pore $K_{2P}2.1$ channel is upregulated in prostate cancer. Furthermore, the calcium-activated intermediate conductance potassium channel $K_{Ca}3.1$ is overexpressed in pancreatic, prostate and breast cancer, as well as in melanomas and lymphomas, whereas the big conductance $K_{Ca}1.1$ channel seems to be upregulated in gliomas, leukemia and prostate and breast cancer cells, respectively. [10, 29, 33, 32]

Regarding lung cancer, as partially mentioned before, the $K_V1.3$ channel, as well as the $K_V11.1$ channel, seem to be expressed in lung cancer cells. Interestingly, the voltage-gated $K_V1.5$ channel seems to be downregulated, whereas the $K_V7.1$ seems to be upregulated in lung cancer cells. It was found, that the two-pore $K_{2P}9.1$, as well as the inward rectifying $K_{ir}3.1$ channel, are upregulated in lung cancer cells and that the calcium-activated potassium

channel $K_{Ca}1.1$ is upregulated in lung primary tumors. Furthermore, three potassium channels ($K_{2P}1.1$, $K_{2P}5.1$, $K_V7.3$) seem to be upregulated and seven ($K_Vb1.3$, K_Vb2, $K_{ir}2.1$, $K_{2P}3.1$, KCNMB4, $K_{Ca}4.2$) seem to be downregulated in lung cancer cells. [23, 29, 33, 32, 10]

3.2.2. Sodium channels

The group of voltage-gated sodium channels consists of nine families ($Na_V1.1$-1.9). Each alpha subunit of the sodium channel links with one or more beta subunit, which can regulate the expression and gating of the channels. A known function of voltage-gated sodium channels is the generation of action potentials in excitable membranes. Moreover, voltage-gated sodium channels are also expressed in non-excitable cells like fibroblasts, immune cells, glia and cancer cells. Local depolarization of the membrane opens the Na_V-channels, which contributes an influx of Na^+-ions into the cell, which in turn causes a depolarization of the whole cell membrane. The most common voltage-gated sodium channel expressed in cancer cells is the $Na_V1.5$ channel, being highly expressed in lymphoma, breast and colon cancer cells. Furthermore, the $Na_V1.2$, $Na_V1.4$ and the $Na_V1.7$ channels are overexpressed in prostate cancer cells. In addition, non-voltage-gated sodium channels, like epithelial sodium channels (ENaCs) and acid-sensitive ion channels (ASICs), which belong to the degenerin/epithelial sodium channel superfamily, are expressed in various tumor cells. [11, 8, 10, 29, 34]

Regarding lung cancer, a study shows that four sodium channel genes (SCN4B, SCN7A, SCNN1B and SCNN1G) are downregulated in lung cancer tissue. [23]

3.2.3. Calcium channels

Voltage-gated calcium channels are expressed in excitable cells as well as in non-excitable cells. In excitable cells, they are responsible for the control of neurotransmitter and hormone secretion, gene expression and many other physiological processes. In non-excitable cells they control cell proliferation and are promising targets for anti-cancer therapy. Typically, these channels consist of five subunits and according to their characteristics and their sensitivity to certain drugs they can be classified into six subgroups: L, N, P, Q, R and T-type channels. Except T-type, which is activated at low voltages, all other types are activated by strong membrane depolarization. Whereas L- ($Ca_V1.1$-1.4) and T-type ($Ca_V3.1$-3.3) channels are expressed in many various cells, the other types are mainly

expressed in neurons. Some types of the T-type channel subfamily are differently expressed in breast, prostate and brain cancer cells. Furthermore, a L-type channel subunit ($Ca_V1.2$) is upregulated in colon cancer cells. A novel study shows that brain tumors, breast, kidney and lung cancer exhibit underexpressed voltage-gated calcium channels, compared with their expression in normal tissue. In addition, it has been detected that other, non-voltage-gated Ca^{2+}-channels are expressed differently and/or have a modified activity in various kind of cancer cells. In particular, literature shows that store-operated Ca^{2+} (SOC) channels are expressed in breast, prostate, pancreas and lung cancer cells. [8, 10, 35, 11, 36, 29]

Since Ca^{2+} signaling is essentially involved in the manifestation of the cell phenotype, proliferation, differentiation, apoptosis and in cells contraction, secretion or excitability, it is important to understand the mechanism behind it. In non-excitable cells, the Ca^{2+}-entry is mainly provided by SOC channels or more precisely, by Ca^{2+} release-activated Ca^{2+} (CRAC) channels, enabling the influx of Ca^{2+} into the cell by emptying the Ca^{2+}-stores of the endoplasmatic reticulum. The depletion of Ca^{2+} in the endoplasmatic reticulum is basically sensed by the stromal interaction molecule STIM1, which activates the store-operated calcium entry (SOCE) by interaction with the pore-forming subunit ORAI1 of the SOC channel. Since ORAI1 is expressed in various types of cells, the SOCE mechanism is an important field of cancer research. In addition, TRP channels participate to apoptosis, since they are particularly involved in controlling the Ca^{2+}-influx into the cell. Furthermore, their expression varies during cancer progression, which indeed makes them attractive for cancer research. TRP channels will be further discussed in 3.2.5. [9, 37, 36]

Regarding lung cancer, a study shows that the $Ca_V1.1$ and $Ca_V1.3$ channel seem to be downregulated in squamous cell carcinoma and that the $Ca_V1.3$ channel is also downregulated in lung adenocarcinoma, but upregulated in lung carcinoid tumors, compared with normal tissue. Furthermore, several researchers found that the T-type $Ca_V3.1$ channel is highly expressed, whereas the $Ca_V3.2$ and the $Ca_V2.3$ channels seem to have a low expression in lung tumors. In NSCLC cells, α7-containing nicotinic acetylcholine receptors are overexpressed. They belong to the class of ligand-gated Ca^{2+}-channels and are thought to contribute to the mitogenic effects of nicotine in lung cancer cells. [8, 10, 31, 35, 38]

3.2.4. Chloride channels

According to their gating mechanism, chloride channels can be classified into three

subgroups [11]:

- Voltage dependent
- Cyclic adenosine monophosphate (cAMP) regulated
- Calcium dependent

Chloride channels are responsible for trans-epithelial secretion, potential hydrogen (pH) and cell volume regulation, proliferation and membrane potential stabilization. The CLC family of ion channels, which comprises the voltage-gated chloride channels, consists of nine different proteins including CLC 1-7, CLCka and CLCkb. Chloride channels of the CLC family have been found in various cancer cells. For example in breast and pancreatic cancer cells, the calcium-activated chloride channel ANO1 seems to be overexpressed, whereas in colorectal cancer cells, three other calcium-activated chloride channels seem to be underexpressed. Since various members of the CLC family are overexpressed in certain cancers and the inhibition of chloride currents results in a reduction of cancer progression, it is obvious that also chloride channels constitute an attractive goal in cancer research. [29, 11]

Regarding lung tumor tissues it has been shown that four chloride channel genes are upregulated (CLCC1, CLCN3, CLCN7, CLIC6) whereas three other chloride channel genes are downregulated (CLIC3, CLIC4, CLIC5) [23].

3.2.5. Non-selective ion channels

Most TRP channels (except TRPV5 and TRPV6, which are exclusively selective for Ca^{2+} ions) do not show selective permeability for specific ions and are not exclusively permeable to Ca^{2+} ions. Principally, they can be classified into seven subgroups [39]:

- Canonical family (TRPC)
- Non-mechanoreceptor potential family (TRPN)
- Melastatin family (TRPM)
- Vanilloid family (TRPV)
- Ankyrin family (TRPA)
- Polycystin family (TRPP)
- Mucolipin family (TRPML9

TRP channels are activated by very diverse mechanisms that range from changes in temperature to changes in pH-value. Another important fact is that TRPN channels do not

occur in mammals. [36, 39]

Regarding cancer, literature shows in general that various TRPC channels are differently expressed in gliomas and prostate cancer cells as well as in lung cancer primary tumors. In particular, the TRPM8, TRPC1 and the TRPV6 channels seem to be upregulated in prostate cancer. TRPV1, TRPV2, TRPM2 and TRPC6 are involved in prostate cancer. Furthermore, TRPC1, TRPC3, TRPC6, TRPM7, TRPM8 and TRPV6 channels seem to be upregulated in breast cancer cells, whereas TRPC1, TRPC3, TRPC4, TRPC6, TRPM7 and TRPM8 are involved in lung cancer. TRPV1 seems to be also upregulated in pancreas primary tumors, whereas TRPM7 and TRPM8 seem to be upregulated in a pancreatic tumor cell line. Finally, TRPV6 is upregulated in colon, ovarian and thyroid tumor too and TRPM8 is upregulated in colon tumors and melanomas. [10, 36, 29, 32, 33]

Concerning lung cancer, a study shows that three members of the TRP-channel family are downregulated (TRPC1, TRPC6, TRPV2), whereas another is upregulated (TRPM2) in cancerous lung tissue [23]. TRPV1 and TRPV6 both seem to be differentially expressed in small cell lung cancer cells, whereas just the former one seems to be expressed in adenocarcinoma [31].

3.3. Ion channels expressed in A549 cells

In order to be able to model the kinetics of voltage gated ion channels in A549 cells, first it is crucial to know which ion channels are expressed in A549 cells.

3.3.1. Potassium Channels

Using polymerase chain reaction (PCR) and Western blot analysis, a study confirmed the mRNA expression and as well, the protein expression of $K_V1.3$ in A549 cells. Via the usage of the selective blocker margatoxin (MgTX) of $K_V1.3$ and as well, specific shRNA, a blockage of A549 cells' proliferation was reached. Therefore, it was suggested that A549 cells express $K_V1.3$ and that selective suppression of the expression inhibits the cells' viability. Roth, who used the selective blocker MgTX as well, confirms this outcome and concludes that the voltage-gated potassium channel $K_V1.3$ is active in A549 cells. [40, 27]

Another study reports that $K_V1.1$ is expressed at mRNA and protein level in A549 cells. The blockage of the channel with Dendrotoxin-κ, a $K_V1.1$ specific blocker, results in an inhibition

of proliferation in A549 cells. This suggests that the channel is involved in cancer cell proliferation. Since the study reports the expression, but not the localization of $K_V1.1$, further research on the subject of localization of $K_V1.1$ in A549 cells was necessary. Results were presented a few years later by partly the same research-group. They reported that $K_V1.1$ is localized in the nuclear fraction of A549 cells. Furthermore, it was found that $K_V1.2$ is localized in the membrane and $K_V2.2$ is localized in the membrane as well as in the nuclear fraction of A549 cells. Concerning the actual topic of the study, the localization of the $K_V1.3$ channel, the results show that a $K_V1.3$ protein expression is detected in the nuclear and cytosolic fraction of A549 cells. [30, 41]

Analyzing with reverse transcription polymerase chain reaction (RT-PCR), another study shows that $K_V9.3$ mRNA is expressed in A549 cells, whereas the protein expression could not be investigated, due to lacking resources. Furthermore, the study shows, that silencing $K_V9.3$ via the usage of siRNA has an anti-proliferative effect on the cells, but it does not induce apoptosis. As $K_V9.3$ is a modifier, or rather silencer, and is not functional on its own, it is not clear whether the channel plays a role in the A549 cells. [42, 43]

As can be seen from another study, RT-PCR and Western Blot analysis show that the voltage gated potassium channels $K_V3.1$, $K_V3.3$, $K_V3.4$ are highly expressed, but also $K_V1.2$, $K_V2.1$ and $K_V9.3$ are expressed in A549 cells [44].

Via RT-PCR, Girault et al. [45] detected the presence of human $K_V7.1$, $K_V10.1$ and $K_V11.1$ mRNA in A549 cells. The exposure to selective blockers shows, that $K_V10.1$ and $K_V11.1$ are not involved, whereas $K_V7.1$ seems to be involved in the regulation of A549 wound healing. Furthermore, they demonstrate that the inhibition of $K_V7.1$ in A549 cells has anti-proliferative effects and impact on the cell cycle progression and cell migration. Additionally, the study suggested that $K_V7.1$ is overexpressed in lung cancer tissues. Due to the small sample of patients, this fact should be treated with caution and needs further investigation. Regarding the $K_V11.1$ channel, another study comes to the result that it is expressed in the human lung cancer cell line A549. Importantly, the study reports that the expression in these cells is the lowest one, compared with four other cancer cell lines. [45, 46]

Besides voltage-gated potassium channels, also some non-voltage-gated potassium channels, including calcium-activated potassium channels, are expressed in A549 cells.

Roth [27] suggests that IK channels are expressed in A549 cells. Furthermore, the study shows that the channel is not by default active. It seems like the channel activity is cell-cycle

dependent and that the channels can be activated, which results in a hyperpolarization of cells. Another study confirms this outcome, since it provides evidence, that there are active $K_{Ca}3.1$ channels in A549 cells, whose blockade reduces A549 cell proliferation and migration. [27, 47]

Ridge et al. [48] identified a BK channel expressed in the A549 cell line, using single-channel patch clamp measurements. The reported channel is activated by membrane depolarization and increased intracellular Ca^{2+} concentration and it has a single-channel conductance of about 242 pS. Due to its large conductance, the channel counts to the "big" or "maxiK" Ca^{2+}-activated K^+ channels. This outcome is confirmed by a study that investigates the behavior of A549 cells in response to changes in alveolar oxygen tension. It confirms the presence of BK channels in A549 cells, where the channels sense acute changes in alveolar oxygen tension. [48, 49]

According to Plummer et al. [50], A549 cells express mRNA of the G-protein inwardly rectifying potassium (GIRK) channels GIRK1, GIRK2, GIRK3 and GIRK4. Since protein and gene expression is needed to form functional GIRK channels, further research would be necessary to ascertain if GIRK channels are expressed and active in A549 cells. [50]

The study of Leithner et al. [51] regarding non-small cell lung cancer cells indicates that A549 cells express functional TASK-1 ($K_{2P}3.1$) channels, which are two-pore domain potassium channels that are usually important for the K^+ efflux and subsequently for the control of the membrane potential of a cell. Furthermore, they suggest that the inhibition of these channels leads to a depolarization and even to an enhanced apoptosis and reduced proliferation in A549 cells. Regarding the potassium two-pore channel TASK-3 ($K_{2P}9.1$) the study reports an expression, but does not consider the activity of the channel. Therefore, it is clear that the channel is expressed in A549 cells, whereas it is not reported, whether the channel is active in this cell line. [51]

3.3.2. Sodium channels

Concerning sodium channels, literature shows that A549 cells do not possess a functional voltage-gated sodium channel. [52, 53]

By way of contrast, acid-sensing ion channels are reported to be expressed in A549 cells. More precisely, a study shows via RT-PCR and Western Blotting that the acid-sensing ion channels ASIC1, ASIC2 and ASIC3 are expressed at mRNA and protein level in A549 cells and

that the inward ASIC-like currents, which are activated by low extracellular pH, in A549 cells are mainly carried by ASIC1 channels. Regarding the localization of the channels, the study shows that ASIC2 is present in the nucleus, whereas ASIC1 and ASIC3 are present in the plasma membrane, the cytoplasm and as well in the nucleus. Furthermore, they show that ASICs are involved in the cells' proliferation and migration induced by extracellular acidosis and that the channels mediate an increase of the intracellular calcium concentration induced by extracellular acidosis. Since the study uses transfected A549 cells, it is not clear if natural A549 cells show the same results. [34]

Besides ASICs, also amiloride-sensitive sodium channels (ENaCs) are expressed in A549 cells, as shown by patch clamp experiments of Lazrak et al. [54]. The results of a study show that the amiloride-sensitive Na^+ currents carried by ENaCs are inwardly rectifying and are neither time- nor voltage dependent. Furthermore, they show that the channel expressed in the cell line has a unitary conductance of 8.6 ± 0.04 pS. [54]

3.3.3. Calcium channels

Researchers reported the expression of $Ca_V3.1$ in lung cancer and anti-proliferative and apoptotic activities for a $Ca_V3.1$ antagonist in A549 cells. Since the location of the expression in the cell, as well as the activity of the channel are not clear and the researchers did not perform any patch clamp experiments, these facts should be treated with caution. [55]

Regarding SOC channels, it was found that STIM1 and ORAI1/CRACM1, which are essential components of the store-operated calcium channel or CRAC, are functionally expressed in A549 cells and that its overexpression inhibits the cell proliferation by attenuation of the store-operated calcium influx. The study confirms mRNA and protein expression via Western Blotting. [56]

3.3.4. Non-selective ion channels

A review reports that the blocking of the TRPC channels TRPC1 and TRPC6 inhibits the proliferation of A549 cells, suggesting that these channels are important goals in lung cancer treatment [36].

Accordingly, Yang et al. [57] found that TRPC6 is highly expressed in various cancer and NSCLC cells. Furthermore, they have found that the blockade of the TRPC6 channel inhibits A549 cell proliferation by cell cycle arrest and that the inhibition of TRPC6 channels reduces

the intracellular Ca^{2+} concentration in A549 cells. Concluding, TRPC6 modulates the intracellular Ca^{2+} concentration in A549 cells by controlling the cell cycle progression. Additionally, they show that TRPC6 is highly expressed at the S-G2/M phase in the cell cycle, rather than at the G1 phase. [57]

Another study regarding TRP channels suggests that TRPV3 is overexpressed in NSCLC cells and that the blockade of TRPV3 leads to an inhibition of A549 cell proliferation. Furthermore, the researchers found that the inhibition of TRPV3 decreases the intracellular calcium concentration of lung cancer cells and in particular of A549 cells. [58]

3.3.5. Summary

In order to summarize this section, all ion channels being expressed and active in A549 cells, as well as their alternative names - as they are quoted on "PubMed Gene", are listed in Table 1 and Table 2.

$K_V1.3$	$K_V3.1$	$K_V3.3$	$K_V3.4$	$K_V7.1$	$K_{Ca}1.1$	$K_{Ca}3.1$
• KCNA3 • MK3 • HGK5 • HLK3 • PCN3 • HPCN3 • HUKIII • potassium voltage-gated channel subfamily A member 3	• KCNC1 • KV4 • EPM7 • NGK2 • potassium voltage-gated channel subfamily C member 1	• KCNC3 • SCA13 • KSHIIID • potassium voltage-gated channel subfamily C member 3	• KCNC4 • C1orf30 • KSHIIIC • HKSHIIIC • potassium voltage-gated channel subfamily C member 4	• KCNQ1 • LQT • RWS • WRS • LQT1 • SQT2 • ATFB1 • ATFB3 • JLNS1 • KCNA8 • KCNA9 • $K_V1.9$ • KVLQT1 • potassium voltage-gated channel subfamily Q member 1	• KCNMA1 • SLO • BKTM • SLO1 • hSlo • MaxiK • PNKD3 • SAKCA • mSLO1 • CADEDS • SLO-ALPHA • bA205K10.1 • potassium calcium-activated channel subfamily M alpha 1	• KCNN4 • IK • IK1 • SK4 • DHS2 • KCA4 • hSK4 • IKCA1 • hKCa4 • hIKCa1 • potassium calcium-activated channel subfamily N member 4

TABLE 1: Ion channels expressed in A549 cells (part 1)

$K_{2P}3.1$	$K_{2P}9.1$	ORAI1	TRPC6	TRPV3	ENaC
• TASK1 • KCNK3 • TASK-1 • OAT1 • PPH4 • TASK • TBAK1 • potassium two pore domain channel subfamily K member 3	• KCNK9 • KT3.2 • TASK3 • TASK-3 • potassium two pore domain channel subfamily K member 9	• IMD9 • TAM2 • ORAT1 • CRACM1 • TMEM142A • calcium release-activated calcium modulator 1	• TRP6 • FSGS2 • transient receptor potential cation channel subfamily C member 6	• OLMS • VRL3 • FNEPPK2 • transient receptor potential cation channel subfamily V member 3	• SCNN1A • BESC2 • ENaCa • SCNEA • SCNN1 • LIDLS3 • ENaCalpha • sodium channel epithelial 1 alpha subunit

TABLE 2: Ion channels expressed in A549 cells (part 2)

3.4. Development of a model approach

Throughout the literature, there is very limited channel-specific information that is suitable to build a model. Therefore, only five specific channels, which are described in sufficient detail in literature, are used for the model approach.

- $K_V1.3$
- $K_{2P}3.1$
- ORAI1
- $K_{Ca}1.1$
- $K_{Ca}3.1$

For the description of voltage-gated ion channels in A549 cells, among others, a Hodgkin-Huxley based model approach is used. Additionally, a contribution of Hou et al. [59] regarding the physiological role of $K_V1.3$ in T-lymphocyte cells serves as a basis for the model approach as it is described below.

As already defined by Hodgkin and Huxley, the total ionic current across a membrane is the sum of all individual ion currents. According to Ohm's law, the ionic current is the product of the membrane conductance times the driving force, as mentioned in equation (3). In order to obtain the specific membrane conductance of a channel, the single-channel conductance has to be multiplied with the number of channels in the membrane. For completing equation (3), the Nernst potential of each channel has to be known.

Since the number of channels in A549 cells is not known, this parameter must be determined experimentally for each channel, which will be described in detail below.

3.4.1. Channel parameters and current equations

The specific channel parameters and their references are listed below in Table 3.

Channel	Single-channel conductance in pS	Nernst potential in mV	Reference
$K_{2p}3.1$	16	-100	[60]
ORAI1	0.01	+80	[61, 59]
$K_V1.3$	15	-73	[59]
$K_{Ca}1.1$	242	-17	[48]
$K_{Ca}3.1$	11	-75	[59]

TABLE 3: Single channel conductances and Nernst potentials of the used channels

Most of the measurements for the determination of the channel parameters are performed at room temperature, but not all researchers quote the temperature the measurements are performed at. There is supportive evidence that temperature affects some channel parameters. In detail, it is reported in literature that the single-channel conductance of the calcium-activated potassium channel $K_{Ca}3.1$ decreases with decreasing temperature and that the Ca^{2+}-sensitivity of the channel increases at lower temperature [62].

Since literature provides parameters for a Hodgkin-Huxley based approach to model the current of the voltage-gated potassium channel $K_V1.3$, the channels' current can be described by the following equation (12):

$$I_{K_V1.3} = g_{K_V1.3} \cdot N_{K_V1.3} \cdot n^4 \cdot (V_m - E_{K_V1.3}) \tag{12}$$

where $g_{Kv1.3}$ is the channels' single-channel conductance, $N_{Kv1.3}$ the number of $K_V1.3$ channels in the membrane, n the gating variable, V_m the membrane potential and $E_{Kv1.3}$ the reversal potential of the $K_V1.3$ channel. With equation (9) as a basis and the following equations (13) and (14) for the steady-state value and the time-constant (obtained from [63]), the gating variable n and thus the current of $K_V1.3$ can be fully described (apart from the number of channels):

$$n_\infty = \frac{1}{1+e^{\frac{V+14.1}{-10.3}}} \tag{13}$$

$$\tau_n = -0.284 \cdot V_m + 19.16 \tag{14}$$

The differential equation obtained when inserting n_∞ and τ_n into equation (9) is solved with the Forward Euler method. It calculates the slope of a given point. The next point of the curve can be found on the tangential line of the previous point. Once this next point is found, a new slope and tangential line can be calculated, which leads to another point. Completing this method over time, it forms a curve that models the actual curve. The Forward Euler method is the simplest numerical integration method, but it is prone to instability and inaccuracy. Since the model is not very complex, the solutions found by Forward Euler method are sufficiently exact.

For the other four channels, a linear approach as it is described in [59] and by equation (3), is chosen to describe the channels' currents, as shown in equation (15)-(18):

$$I_{K_{2P}3.1} = g_{K_{2P}3.1} \cdot N_{K_{2P}3.1} \cdot (V_m - E_{K_{2P}3.1}) \tag{15}$$

$$I_{ORAI1} = g_{ORAI1} \cdot N_{ORAI1} \cdot (V_m - E_{ORAI1)} \tag{16}$$

$$I_{K_{Ca}1.1} = g_{K_{Ca}1.1} \cdot N_{K_{Ca}1.1} \cdot (V_m - E_{K_{Ca}1.1}) \tag{17}$$

$$I_{K_{Ca}3.1} = g_{K_{Ca}3.1} \cdot N_{K_{Ca}3.1} \cdot (V_m - E_{K_{Ca}3.1}) \tag{18}$$

Finally, the total ionic current across the membrane of A549 cells is determined by:

$$I_{ion} = I_{K_V1.3} + I_{K_{2P}3.1} + I_{ORAI1} + I_{K_{Ca}1.1} + I_{K_{Ca}3.1} \tag{19}$$

3.4.2. Number of channels

The basis of the model of A549 cells is a patch clamp measurement between -60 mV and +60 mV. It is known that the whole-cell current at + 60 mV membrane voltage is about 1 nA and that it is slightly negative at – 60 mV, which is the only benchmark for the development of the model approach.

With Matlab (Mathworks Inc., Natick, USA), the total ionic current is simulated at membrane voltages between -60 mV and +60 mV. Since all parameters, except the number of channels are known, the total ionic current is modelled by adapting the number of channels for each of the five previously mentioned channels. The number of channels is adjusted in a way, such that the total ionic current is about 1 nA at +60 mV. Literature does not serve any information concerning the number of channels in A549 cells or in lung cancer cells in general. The only approximate benchmark regarding the number of channels is shown in the previously mentioned paper of Hou et al. [59] with $N_{Kv1.3} \approx 300$ and $N_{Kca3.1} \approx 10$ for a T-lymphocyte cell.

When the intended current of 1 nA at +60 mV is reached, the model can be used to simulate the kinetics of A549 cells when specific channels are blocked.

4. Results

4.1. Patch Clamp Experiments

Figure 2 shows an exemplary current-time curve of A549 cells. The currents were obtained by patch clamp measurements and a voltage-step protocol between -60 mV and +60 mV in 10 mV steps. As suggested by Roth [27] and indicated in Figure 2, the currents can be kinetically separated into two different parts – an instantaneously activating (I_{inst}) and a time-dependent (I_{td}) one. The corresponding current-voltage curve is obtained by plotting the steady-state current of each voltage-step against voltage, as can be seen exemplarily in Figure 3.

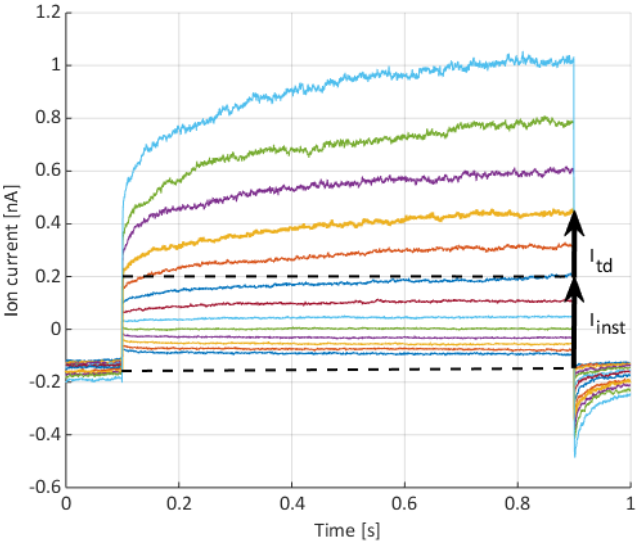

FIGURE 2: Exemplary current-time curve of A549 cells

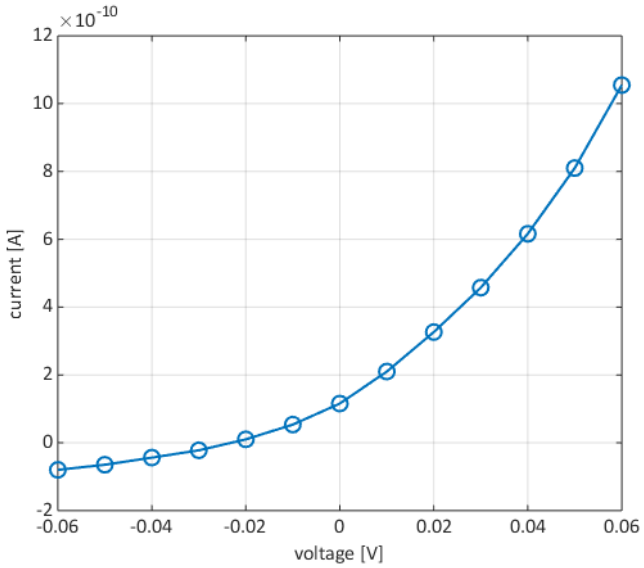

FIGURE 3: Exemplary current-voltage curve of A549 cells

4.2. Model Experiments

Table 4 shows the number of channels resulting together in a total ionic current of about 1 nA at +60 mV. Figure 4 and Figure 5 show the I/V-curves of the individual currents, as well as the curves of the measured and the modelled total ionic currents. In order to be able to compare the measured total ionic current of A59 cells with the modelled one, the measured (reference) current is plotted as red line in each of the following figures.

Channel	Number
$K_{2P}3.1$	80
ORAI1	100
$K_V1.3$	180
$K_{Ca}1.1$	20
$K_{Ca}3.1$	60

TABLE 4: Original number of channels

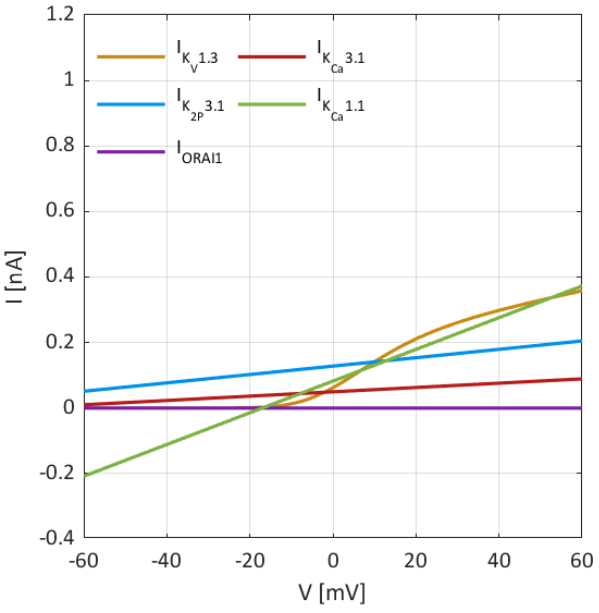

FIGURE 4: IV-curves of the original single currents

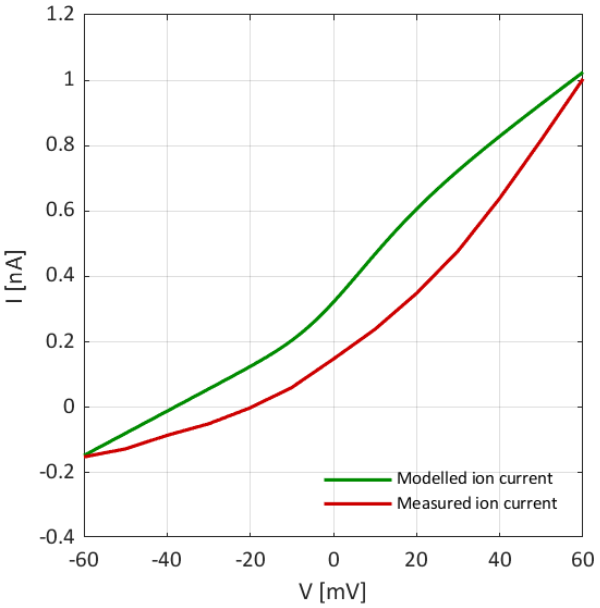

FIGURE 5: IV-curves of the measured and the modelled total ionic current

Table 5 shows the number of channels when the $K_{2P}3.1$ channel is blocked (i.e., when it is set to zero). Figure 6 and Figure 7 show the corresponding I/V-curves of the individual currents and the total ionic current when the $K_{2P}3.1$ channel is blocked.

Channel	Number
$K_{2P}3.1$	0
ORAI1	100
$K_V1.3$	180
$K_{Ca}1.1$	20
$K_{Ca}3.1$	60

TABLE 5: Number of channels when the $K_{2P}3.1$ channel is blocked

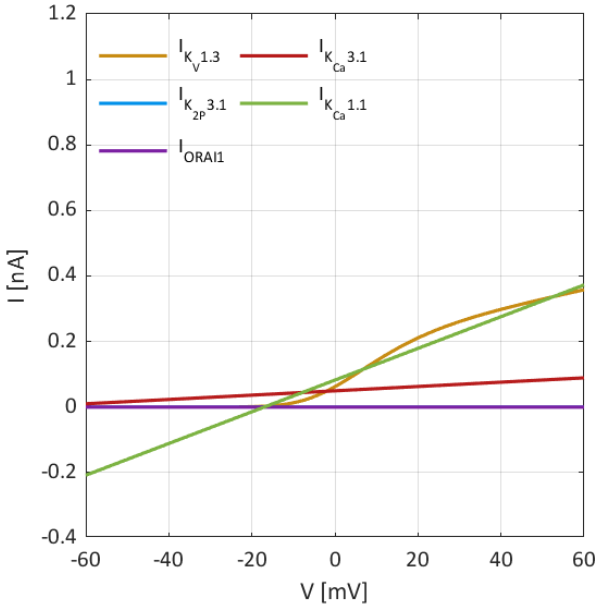

FIGURE 6: IV-curves of the single currents when the $K_{2P}3.1$ channel is blocked

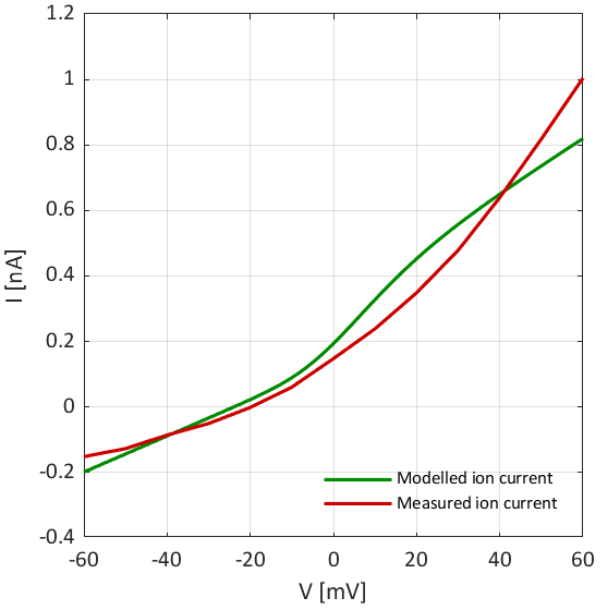

FIGURE 7: IV-curves of the modelled total ionic current when the $K_{2P}3.1$ channel is blocked and the reference current

Table 6 shows the number of channels when the ORAI1 channel is blocked (i.e., when it is set to zero). Figure 8 and Figure 9 show the corresponding I/V-curves of the individual currents and the total ionic current when the ORAI1 channel is blocked.

Channel	Number
$K_{2P}3.1$	80
ORAI1	0
$K_V1.3$	180
$K_{Ca}1.1$	20
$K_{Ca}3.1$	60

TABLE 6: Number of channels when the ORAI1 channel is blocked

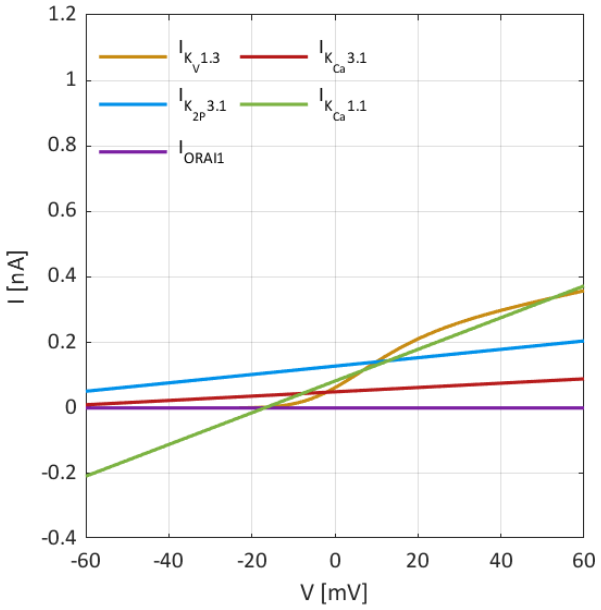

FIGURE 8: IV-curves of the single currents when the ORAI1 channel is blocked

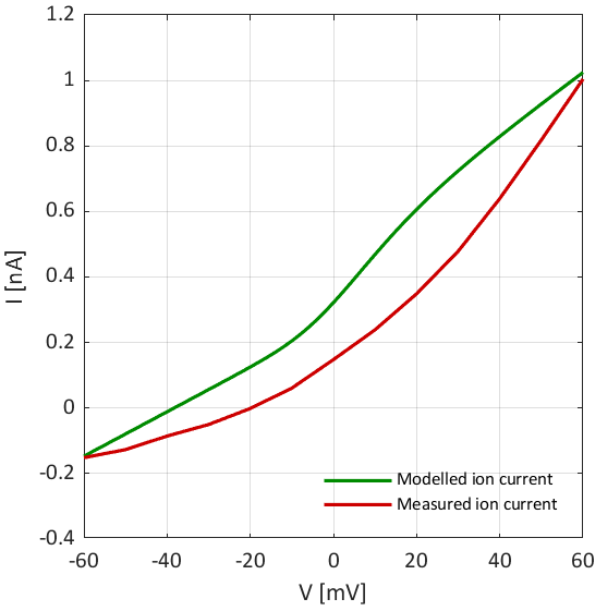

FIGURE 9: IV-curves of the modelled total ionic current when the ORAI1 channel is blocked and the reference current

Table 7 shows the number of channels when the $K_V1.3$ channel is blocked (i.e., when it is set to zero). Figure 10 and Figure 11 show the corresponding I/V-curves of the individual currents and the total ionic current when the $K_V1.3$ channel is blocked.

Channel	Number
$K_{2P}3.1$	80
ORAI1	100
$K_V1.3$	0
$K_{Ca}1.1$	20
$K_{Ca}3.1$	60

TABLE 7: Number of channels when the $K_V1.3$ channel is blocked

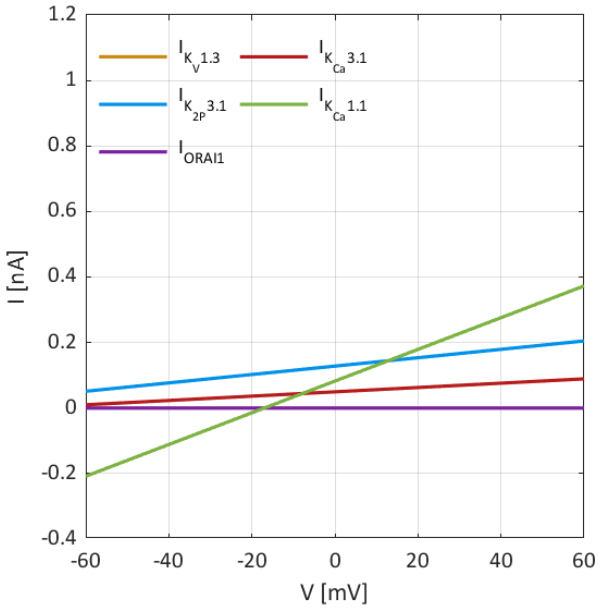

FIGURE 10: IV-curves of the single currents when the $K_V1.3$ channel is blocked

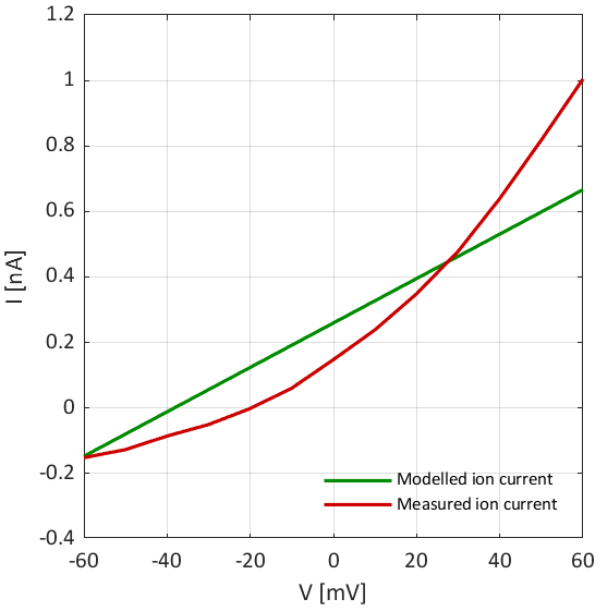

FIGURE 11: IV-curves of the modelled total ionic current when the $K_V1.3$ channel is blocked and the reference current

Table 8 shows the number of channels when the $K_{Ca}1.1$ channel is blocked (i.e., when it is set to zero). Figure 12 and Figure 13 show the corresponding I/V-curves of the individual currents and the total ionic current when the $K_{Ca}1.1$ channel is blocked.

Channel	Number
$K_{2P}3.1$	80
ORAI1	100
$K_V1.3$	180
$K_{Ca}1.1$	0
$K_{Ca}3.1$	60

TABLE 8: Number of channels when the $K_{Ca}1.1$ channel is blocked

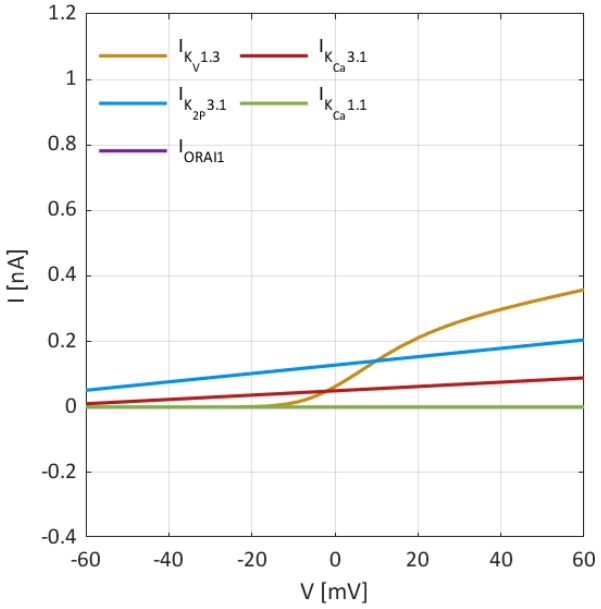

FIGURE 12: IV-curves of the single currents when the $K_{Ca}1.1$ channel is blocked

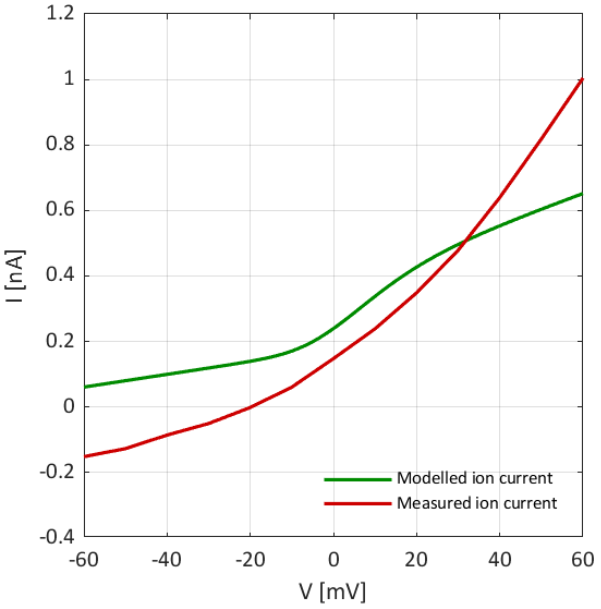

FIGURE 13: IV-curves of the modelled total ionic current when the $K_{Ca}1.1$ channel is blocked and the reference current

Table 9 shows the number of channels when the $K_{Ca}3.1$ channel is blocked (i.e., when it is set to zero). Figure 14 and Figure 15 show the corresponding I/V-curves of the individual currents and the total ionic current when the $K_{Ca}3.1$ channel is blocked.

Channel	Number
$K_{2P}3.1$	80
ORAI1	100
$K_V1.3$	180
$K_{Ca}1.1$	20
$K_{Ca}3.1$	0

TABLE 9: Number of channels when the $K_{Ca}3.1$ channel is blocked

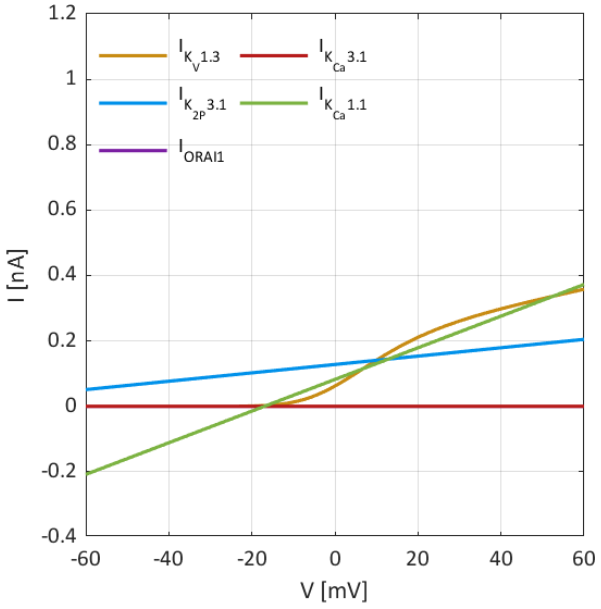

FIGURE 14: IV-curves of the single currents when the $K_{Ca}3.1$ channel is blocked

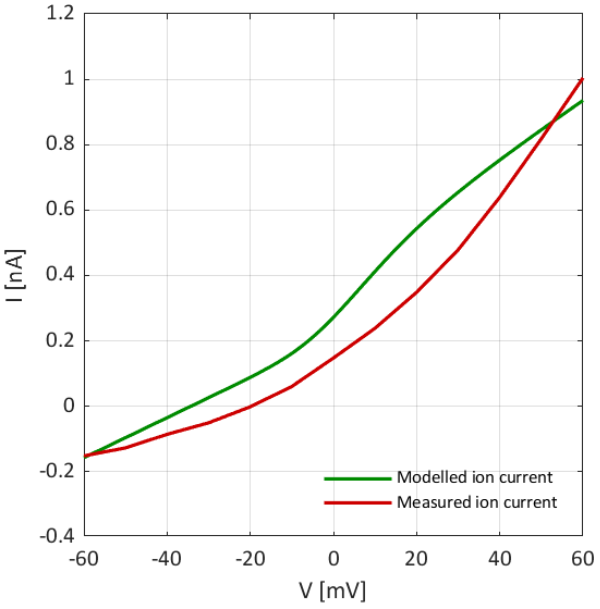

FIGURE 15: IV-curves of the modelled total ionic current when the $K_{Ca}3.1$ channel is blocked and the reference current

Table 10 shows the number of channels when the voltage-gated channels are blocked (i.e., when $K_V1.3$ and $K_{Ca}1.1$ are set to zero). Figure 16 and Figure 17 show the corresponding I/V-curves of the individual currents and the total ionic current when the voltage-gated channels are blocked.

Channel	Number
$K_{2P}3.1$	80
ORAI1	100
$K_V1.3$	0
$K_{Ca}1.1$	0
$K_{Ca}3.1$	60

TABLE 10: Number of channels when the voltage-gated channels are blocked

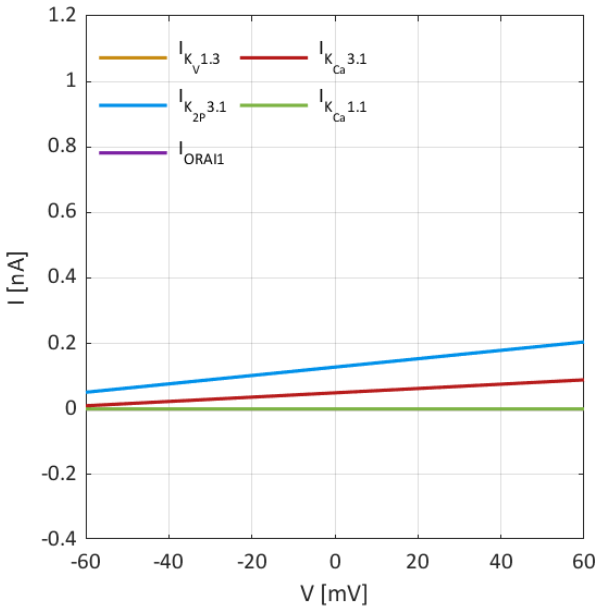

FIGURE 16: IV-curves of the single currents when the voltage-gated channels are blocked

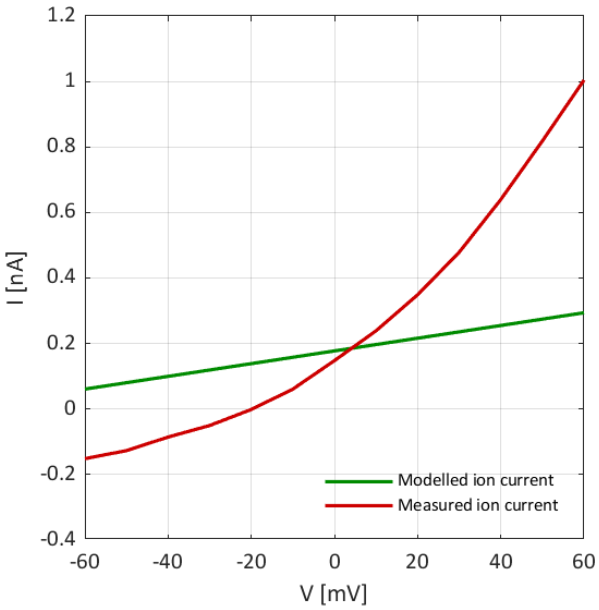

FIGURE 17: IV-curves of the modelled total ionic current when the voltage-gated channels are blocked and the reference current

Table 11 shows the number of channels when the voltage-gated channels and the $K_{2P}3.1$ channel are blocked (i.e., when $K_V1.3$, $K_{Ca}1.1$ and $K_{2P}3.1$ are set to zero). Figure 18 and Figure 19 show the corresponding I/V-curves of the individual currents and the total ionic current.

Channel	Number
$K_{2P}3.1$	0
ORAI1	100
$K_V1.3$	0
$K_{Ca}1.1$	0
$K_{Ca}3.1$	60

TABLE 11: Number of channels when the voltage-gated and $K_{2P}3.1$ channels are blocked

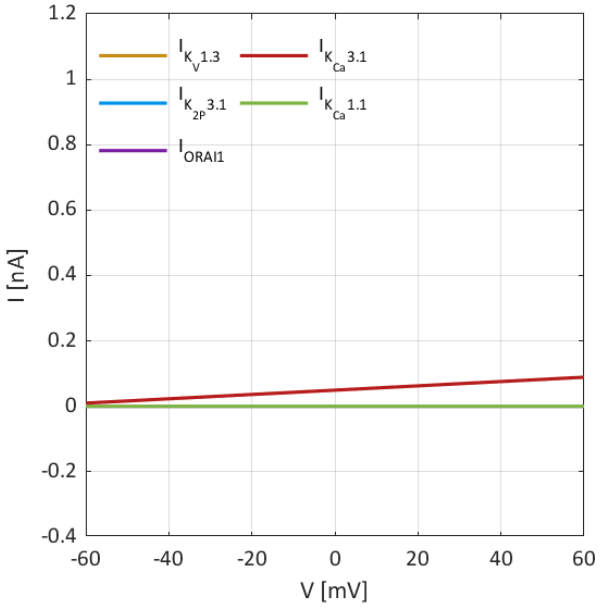

FIGURE 18: IV-curves of the single currents when the voltage-gated and $K_{2P}3.1$ channels are blocked

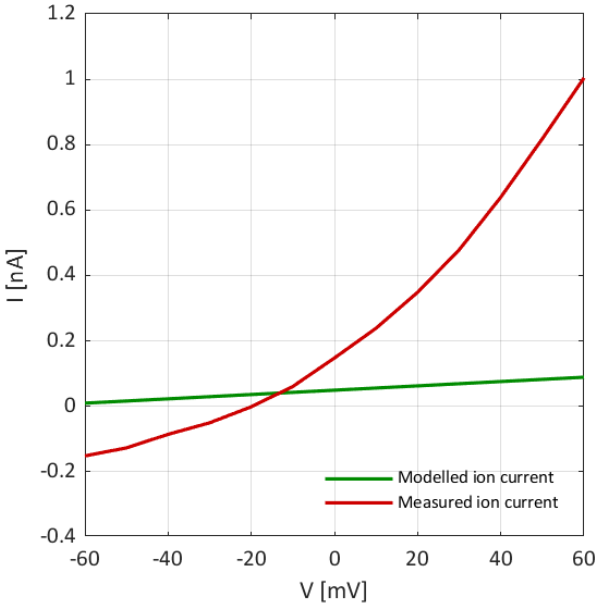

FIGURE 19: IV-curves of the modelled total ionic current when the voltage-gated and $K_{2P}3.1$ channels are blocked and the reference current

5. Discussion

5.1. Ion channel expression in A549 cells

The results with the original number of channels, as can be seen in Figure 5, show an I/V-curve that is similar to the one of whole-cell patch clamp measurements of A549 cells. Nevertheless, the main drawback of the present model is the limited number of included ion channels. Since literature shows very contentious, or even no information at all (e.g. chloride channels) regarding the expression and localization of the specific channels, it is often not clear, whether a channel is really expressed in the cell membrane of A549 cells. For some channels, an expression is only reported for the nucleus or for the cytosol and not for the plasma membrane. Furthermore, the confirmation of channel expression does not mean that the channel is active and thus that it contributes to the electrical behavior of the cell. Consequently, further research regarding the expression and the activity of ion channels in A549 cells has to be accomplished in order to understand the cells' behavior and the interaction between the entirety of functional expressed channels. The five channels mentioned in chapter 3.4 are chosen, because it seems that they are expressed and active in A549 cells. Moreover, there are enough parameters and information available in literature to fully describe the currents of these channels. In fact, several other channels seem to be expressed in A549 cells, but there is not enough information available to fully describe the currents and thus to implement them into the model.

Indeed, literature reports a contradictory localization of the voltage-gated potassium channel $K_V1.3$. Nevertheless, the channel is assumed to be expressed in the cell membrane of A549 cells too, since Roth, who reported an expression in the plasma membrane, also confirmed this with several patch clamp experiments and blockers [27]. Although no information regarding the localization of the other four channels could be found, they were incorporated into the model, as there exist representable patch clamp experiments for all of the channels. As a result, it can be assumed that the ion channels are expressed and active in the cell membrane.

The expression of the voltage-gated potassium channel $K_V11.1$ in A549 cells is also subject of controversial discussion in literature. Since there exist no more detailed information or results of patch clamp experiments, further research is necessary to confirm the expression

of the channel and thus to make it implementable into the model.

In contrast to other cells, A549 cells do not possess active voltage-gated sodium channels. This may be due to the cytosolic expression of the channels, as suggested by a French research group [52]. Since A549 cells are weakly metastatic, this would confirm the assumption that the functional expression of voltage-gated sodium channels is an integral component of the metastatic process in NSCLC cells.

5.2. Model approach

While researching, only for the voltage-gated potassium channel $K_V1.3$ a more or less detailed model approach could be found in literature. For that reason, only the current of this specific channel was described by a Hodgkin-Huxley based approach. Contrarily, the other channels were described according to Ohm's law with a linear approach. In addition, the paper of Hou et al. [59] covers channels of T-lymphocytes, which are non-excitable cells (like A549 cells) and express partly the same channels as A549 cells. Therefore, the linear description of some of the channels' currents can be used to describe some of the channels that are expressed in A549 cells.

Another major limitation of the model is the missing inclusion of the calcium concentration. Since the calcium-activated potassium channel $K_{Ca}3.1$ is solely activated by intracellular calcium, it would require a calcium-dependent equation for a more exact description of the provoked current. The same applies to the calcium-activated potassium channel $K_{Ca}1.1$, which is indeed voltage-dependent, but can be also activated by intracellular calcium. A possible approach to include these two channels into the model is the one of Italian researchers where a hypothetical model for the description of an intermediate calcium-activated potassium channel is built [64]. Due to missing cell-specific parameters and according to the fact that, it is not clear yet, for which cells the model is applicable, it is not included in the present model approach to describe the kinetics of A549 cells.

The linear description of the store-operated channel ORAI1 is another limitation, since this channel is activated by depletion of intracellular calcium stores. Therefore, also for this channel, the calcium concentration must be included in a way that the current can be described more exactly.

Similarly, also the current of the potassium two-pore channel $K_{2P}3.1$ could be described in

more detail, as this channel is sensitive to extracellular pH. Thus, an implementation of the cells' pH may lead to a better description of this current.

One of the most important facts to know for the description of the channels is their single channel conductance. Literature reports values of about 0.1 to 100 pS for the single channel conductance of typical ion channels. Obviously, the values for the maxiK channel $K_{Ca}1.1$ and the one for ORAI1 are not in this range. Due to the small single-channel conductance of ORAI1, the current of this channel is quite small.

Since there is providing evidence that temperature affects various channel properties, the temperature dependence of the ion channels must be included in the model in order to achieve a higher accuracy. Temperature dependent changes of channel parameters can be described by the temperature coefficient Q_{10}, which depicts the relative increase of a parameter when the temperature increases by 10°C. The Q_{10} coefficient is very high when the channel is very sensitive to temperature, as for example for thermosensitive TRP channels. In principal, temperature is relevant for all ion channels, like e.g. voltage-gated ion channels, even if their Q_{10} coefficient is much smaller than for TRP channels that are sensitive to temperature. In order to be able to include the temperature dependency into the model, further research on the temperature-dependent behavior of specific channels is needed. One possible way to obtain a temperature dependent model would be to include the temperature coefficient, once known, to every single current by multiplying it with the voltage-dependent rate coefficients α and β of a Hodgkin-Huxley type model approach. However, more accurate temperature dependencies could be obtained by finding thermodynamic parameters for each current, like e.g. Destexhe and Huguenard [65] provided a few years ago for thalamic neurons. [7]

5.3. Results of model experiments

As can be seen in Figure 4 and Figure 5, the general shape of the I/V-curve is mainly caused by the current of the voltage-gated potassium channel $K_V1.3$, as it is the only current that is modelled by a Hodgkin-Huxley approach. Obviously, the maxiK channel $K_{Ca}1.1$ causes the negative part of the total ionic current in regions of lower voltage, with it being the only single channel current that is partly negative. The currents of the channels $K_{Ca}3.1$ and $K_{2P}3.1$ contribute to the total ionic current in an amplifying way, as well as ORAI1, where the

amplifying effect is quite small, however.

Regarding the number of channels, it can be seen in Table 4 that $K_V1.3$ channels make up the largest part of all channels considered in the model. This coincides with the relatively large number of $K_V1.3$ channels compared to the number of $K_{Ca}3.1$ channels reported by Hou et al. [59], as mentioned above. The number of $K_{Ca}1.1$ channels was chosen in a way such that the total ionic current is slightly negative at -60 mV. As the current of ORAI1 is very small, the variation of the channel number does not have a great effect on the total ionic current. The number of the other channels was chosen in a way such that the amplifying effect is strong enough to reach a value of approximately 1 nA at +60 mV.

Figure 6 and Figure 7 show the I/V-curve with a blocked $K_{2P}3.1$ channel. It is evident that the total current is lower over the entire voltage range than in the original state of the model, which is logical due to the missing amplifying factor of $K_{2P}3.1$. The same applies to $K_{Ca}3.1$, as can be seen in Figure 14 and Figure 15.

Figure 8 and Figure 9 show that the blockage of ORAI1 has almost no effect on the total ionic current. This is due to the very small single channel current of ORAI1.

In contrast, the blockage of $K_V1.3$ has a huge effect on the shape of the I/V-curve of the total ionic current, as depicted in Figure 10 and Figure 11. Since the single channel current of $K_V1.3$ increases at voltages above -20 mV, it is obvious that the total ionic current in this voltage range is lower with blocked $K_V1.3$ channels than the original one. Furthermore, it can be clearly seen in Figure 11 that the I/V-curve of the total ionic current with blocked $K_V1.3$ channels is linear, due to the missing Hodgkin-Huxley type part of the current. Roth [27] reported that the current density is reduced by 61% at +60 mV when blocking the $K_V1.3$ channel with MgTX. Furthermore, it was reported that an instantaneous current, (exemplarily indicated in Figure 2) is reduced by 89% at + 40 mV by using the blocker Clotrimazole (CLT) as a specific inhibitor of hIK type potassium channels. Roth concluded that the instantaneously activating part of the current is dominated by hIK channels. Obviously, as seen in Figure 11, the total ionic current in the model is reduced by around 40 % at +60 mV if the $K_V1.3$ channel is blocked. Regarding the hIK channel, it can be seen in Figure 15 that the blockage of the channel in the model results in a much lower reduction of the total ionic current than reported in literature, as described above. A possible explanation for the discrepancies would be that Roth [27] takes an instantaneously activating current as initial current. Therefore, the percentage reduction of the current is bigger than the one with the

total ionic current serving as initial current. In addition, it was reported that the blocker CLT also inhibits parts of the time dependent current, which seems to be caused by a slowly-activating outward rectifier channel. The nature of this channel remains unknown in the contribution of Roth. Since $K_{2P}3.1$ is an outward rectifying potassium channel, it might be that this channel is the reported outward rectifying one. However, further research regarding the sensitivity of $K_{2P}3.1$ to CLT is necessary to confirm this assumption. Furthermore, CLT is also able to block TRP channels, and to be more precisely it is able to block the TRPC6 channel that is also expressed in A549 cells. Therefore, further research regarding the behavior of TRPC6 channels may reveal interesting results concerning the above mentioned unknown channel. [27, 66]

As can be seen in Figure 12 and Figure 13, the blockage of the maxiK channel $K_{Ca}1.1$ results in a lower total ionic current, since the single channel current of $K_{Ca}1.1$ is an amplifying factor. Apart from that, the total ionic current has no negative portion if this channel is blocked, which is evidently, since the current of $K_{Ca}1.1$ is the only one of the five used that is partially negative in the voltage range between -60 and +60 mV.

In Figure 16 and Figure 17, it can be seen that the blockage of the voltage-gated channels $K_V1.3$ and $K_{Ca}1.1$ results in a strong reduction of the total ionic current. Furthermore, the total ionic current has no negative part anymore. The reason for blocking exactly these channels is that Leithner et al. [51] applied a holding potential of 0 mV when performing patch clamp measurements with A549 cells, which inactivates the voltage-gated potassium channels. They called the remaining current non-inactivating potassium current and plot it as an I/V-curve in a voltage-range between - 100 and + 60 mV. However, it is very difficult to obtain absolute values out of the I/V-curve. Nevertheless, it can be clearly seen that the total ionic current (illustrated in Figure 17) is higher than the non-inactivating potassium current at a pH of 7.3 from the paper. Since the current from the paper at a pH of 8.3 seems to be approximately the same as the current from Figure 17, the implementation of pH to the model would serve an explanation for the different IV-curves. Another possible explanation would be the limited amount of channels that is implemented in the model. In Figure 18 and Figure 19, the I/V-curves are depicted, where in addition to the voltage-gated potassium channels the $K_{2P}3.1$ channel is also blocked. These plots were created in order to be able to compare them with the plots of the above-mentioned paper, since Leithner et al. [51] have performed measurements using the selective $K_{2P}3.1$ inhibitor anandamide. Again, it is very

difficult to obtain absolute values from the I/V-curve of the paper, but anyway, it can be seen that the remaining current (with inhibited $K_{2P}3.1$ channel) from the paper is slightly higher than the current shown in Figure 19. A possible explanation for this would be that the linear description of the $K_{2P}3.1$ current is not exact enough, as already discussed above. [51]

5.4. Outlook

The present thesis is an attempt to develop a reasonable model that describes the kinetics of A549 cells. The model could be improved, i.e. by performing single-channel measurements to have a better understanding to what extent the specific channels are expressed in A549 cells. Furthermore, single channel measurements could help to obtain the missing channel specific parameters of the channels that are not yet included in the present model.

Adding implementations of temperature, calcium concentration and pH would increase the validity of the model. A temperature dependent model can be obtained by implementing either a temperature coefficient or thermodynamic parameters. Performing single-channel measurements at different temperature conditions might lead to a better simulation of the temperature-dependent electrophysiological behavior.

In conclusion, including further channels that are expressed in A549 cells and the consideration of their kinetics and specific activation characteristics would serve a much more exact model.

6. Conclusion

In this thesis, the effects of single channel kinetics on the whole current response of the human adenocarcinomic alveolar basal epithelial cell line A549 were studied by developing a model approach. By thorough literature research, it was possible to identify ion channels that are expressed in A549 cells. Subsequently, some of the ion channels that are expressed in A549 could be described in a way that they are implementable into the model.

The five ion channels $K_V1.3$, $K_{2P}3.1$, ORAI1, $K_{Ca}1.1$ and $K_{Ca}3.1$ were incorporated into the model. Due to missing channel specific model parameters, only the voltage-gated potassium channel $K_V1.3$ is described by a Hodgkin-Huxley based approach. Contrarily, the other four channels are described according to Ohm's law, i.e. with a linear approach. Since the quantities of the various channels have not been described in literature yet, these parameters were adjusted in a way such that the total ionic current matches with the measured current from patch clamp measurements of A549 cells. The model serves I/V-curves of the individual ion currents, as well as of the total ionic current for a voltage range between -60 and +60 mV.

By adapting the number of channels and in particular by setting the quantity of a specific channel to zero, the blockage of individual channels can be simulated. Regarding the number of channels, it can be seen that $K_V1.3$ channels make up the largest part of all channels considered in the model. This coincides with the relatively large number of $K_V1.3$ channels compared to the number of $K_{Ca}3.1$ channels in T-cells, as reported in literature.

As a result, it was revealed that the calcium-activated potassium channel $K_{Ca}1.1$ is responsible for the negative part of the total ionic current in lower voltage ranges. Obviously, the voltage-gated potassium channel $K_V1.3$ is accountable for the shape of the IV-curve, since it is the only current that is modelled in a non-linear way. The other three channels $K_{Ca}3.1$, $K_{2P}3.1$ and ORAI1 contribute to the total ionic current in an amplifying way.

Major limitations of the present model are the limited variety of channels implemented into the model, as well as the missing consideration of calcium concentration, temperature and pH-value. Therefore, further research regarding ion channel expression in A549 cells, single channel behavior and temperature dependence of these channels may reveal interesting new insights into cancer electrophysiology.

7. References

[1] A. Molleman, Patch Clamping - An Introductory Guide to Patch Clamp Electrophysiology, West Sussex: John Wiley & Sons Ltd, 2003.

[2] B. Hille, Ion Channels of Excitable Membranes, Sunderland, Massachusetts U.S.A.: Sinauer Associates, Inc., 2001.

[3] D. Silbernagl, Color Atlas of Physiology 6th edition, Stuttgart, New York: Thieme, 2009.

[4] W. J. Brackenbury and M. Yang, "Membrane potential and cancer progression," *frontiers in physiology,* 17 July 2013.

[5] L. H. Schmidt, Physiologie des Menschen mit Pathophysiologie 31. Auflage, Würzburg/Tübingen: Springer, 2010.

[6] F. H. Yu, V. Yarov-Yarovoy, G. A. Gutman and W. A. Catterall, "Overview of Molecular Relationships in the Voltage-Gated Ion Channel Superfamily," *Pharmalogical Reviews Vol. 57, No.4,* pp. 387-395, 2005.

[7] D. Sterratt, B. Graham, A. Gillies and D. Willshaw, Principles of Computational Modeling in Neuroscience, Cambridge: Cambdrige University Press, 2011.

[8] J. L. Fiske, V. P. Fomin, M. L. Brown, R. L. Duncan and R. A. Sikes, "Voltage-sensitive ion channels and cancer," *Cancer Metastasis Rev,* pp. 493-500, 2006.

[9] V. Lehen'kyi, G. Shapovalov, R. Skryma and N. Prevarskaya, "Ion channnels and transporters in cancer. 5. Ion channels in control of cancer and cell apoptosis," *American Journal of Cell Physiology,* p. 9, 21 September 2011.

[10] W. Brackenbury, "Ion channels in cancer," in *Ion channels in health and disease*, Academic Press, 2016, p. 392.

[11] V. R. Rao, M. Perez-Neut, S. Kaja and S. Gentile, "Voltage-Gated Ion Channels in Cancer Cell Proliferation," *Cancers,* pp. 849-875, 22 May 2015.

[12] M. A. Rana, N. Yao, S. Mukhopadhyay, F. Zhang, E. Warren and C. Payne, "Modeling the effect of nanoparticles & the bistability of transmembrane potential in non-excitable cells," in *American Control Conference (ACC)*, Boston, MA, USA, 2016.

[13] A. Hodgkin and A. Huxley, "A quantitative description of membrane current and its application to conduction and excitation in nerve," *J. Physiol.,* no. 117, pp. 500-544, March 1952.

[14] M. Nelson, "Electrophysiological Models," in *Databasing the Brain: From Data to Knowledge*, New York, Wiley, 2004.

[15] Y. Okada, Patch Clamp Techniques From the Beginning to Advanced Protocoles, Springer, 2012.

[16] M. Martina and S. Taverno, Patch-Clamp Methods and Protocols, New York: Springer, 2014.

[17] W. Walz, Patch-Clamp Analysis Advanced Techniques, New Jersey: Human Press, 2007.

[18] H. N. Rubaiy, "A Short Guide to Electrophysiology and Ion Channels," *J Pharm Pharm Sci,* pp. 48-67, 17 March 2017.

[19] M. Malboubi and K. Jiang, Gigaseal Formation in Patch Clamping - With Applications of Nanotechnology, London: Springer, 2014.

[20] E. P. O'Keefe, "siRNAs and shRNAs: Tools for Protein Knockdown by Gene Silencing,"

MATER METHODS, 2013.

[21] 2017. [Online]. Available: https://www.cellbiolabs.com/sites/default/files/AKR-209-gfp-a549-cell-line.pdf. [Accessed 18 June 2018].

[22] C. Zappa and S. A. Mousa, "Non-small cell lung cancer - current treatment and future advances," *Translational Lung Cancer Research,* pp. 288-300, 25 May 2016.

[23] J.-H. Ko, W. Gu, I. Lim, ,. H. Bang, E. A. Ko and T. Zhou, "Ion Channel Gene Expression in Lung Adenocarcinoma: Potential Role in Prognosis and Diagnosis," *PLOS ONE,* pp. 1-12, 23 January 2014.

[24] K. Wang, Y. Zhao, D. Chen, B. Fan, Y. Lu, L. Chen, R. Long, J. Wang and C. Jian, "Data Descriptor: Specific membrane capacitance, cytoplasm conductivity and instantaneous Young's modulus of single tumour cells," *Scientific Data,* 14 February 2017.

[25] R.-D. Jiang, H. Shen and Y.-J. Piao, "The morphometrical analysis on the ultrastructure of A549 cells," *Romanian Journal of Morphology and Embryology,* pp. 663-667, 2010.

[26] X. Liang and Y. Huang, "Intracellular Free Calcium Concentration and Cisplatin Resistance in Human Lung Adenocarcinoma A549 Cells," *Bioscience Reports,* pp. 129-138, 11 May 2000.

[27] B. Roth, "Exposure to sparsely and densely ionizing irradiation results in an immediate activation of K+ channels in A549 cells and in human peripheral blood lymphocytes," Technische Universität Darmstadt, Darmstadt, 2014.

[28] L. Catacuzzeno and F. Franciolini, "Role of KCa3.1 Channels in Modulating Ca2+ Oscillations during Glioblastoma Cell Migration and Invasion," *International Journal of Molecular Sciences,* 29 September 2018.

[29] E. Lastraioli, J. Iorio and A. Arcangeli, "Ion channel expression as promising cancer biomarker," *Biochimica et Biophysica Acta,* pp. 2685-2702, 16 December 2014.

[30] S. H. Jang, P. D. Ryu and S. Y. Lee, "Dendotoxin-k suppresses tumor growth induced by human lung adenocarcinoma cells in nude mice," *Journal of Vetinary Science,* pp. 35-40, 2011.

[31] L. Leanza, A. Managò, M. Zoratti, E. Gulbins and I. Szabo, "Pharmacological targeting of ion channels for cancer therapy: In vivo evidences," *Biochimica et Biophysica Acta,* pp. 1385-1397, 30 November 2016.

[32] O. Bogin, "Ion Channels and Cancer - An updated overview," *Modulator,* 2004.

[33] R. Schönherr, "Clinical relevance of Ion Channels for Diagnosis and Therapy of Cancer," *The Journal of Membrane Biology,* pp. 175-184, 9 September 2005.

[34] Y. Wu, B. Gao, Q.-J. Xiong, Y.-C. Wang, D.-K. Huang and W.-N. Wu, "Acid-sensing ion channels contribute to the effect of extracellular acidosis on proliferation and migration of A549 cells," *Tumor Biology,* pp. 1-8, June 2017.

[35] N. N. Phan, C.-Y. Wang, C.-F. Chen, Z. Sun, M.-D. Lai and Y.-C. Lin, "Voltage-gated calcium channels: Novel targets for cancer therapy," *Oncology Letters,* pp. 2059-2074, 13 April 2017.

[36] N. Déliot and B. Constantin, "Plasma membrane calcium channels in cancer: Alterations and consequences for cell proliferation and migration," *Biochimica et Biophysica Acta,* pp. 2512-2522, 2 June 2015.

[37] H. Yang, Q. Zhang, J. He and W. Lu, "Regulation of calcium signaling in lung cancer," *Journal of Throacic Disease,* pp. 52-56, 15 February 2010.

[38] A. Suo, A. Childers, ,. A. D'Silva, L. F. Petersen, S. Otsuka, M. Dean, H. Li, E. K. Enwere, B. Pohorelic, A. Klimowicz, I. A. Souza, J. Hamid, G. W. Zamponi and D. Bebb, "Cav3.1 overexpression is associated with negative characteristics and prognosis in non-small cell lung cancer," *Oncotarget,* pp. 8573-8583, 12 January 2018.

[39] K. Venkatachalam and C. Montell, "TRP Channels," *Annual Review of Biochemistry,* pp. 387-417, 2007.

[40] S. H. Jang, S. Y. Choi, P. D. Ryu and S. Y. Lee, "Anti-proliferative effect of Kv1.3 blockers in A549 human lung adenocarcinoma in vitro and in vivo," *European Journal of Pharmacology,* pp. 26-32, 29 October 2010.

[41] S. H. Jang, J. K. Byun, W.-I. Jeon, S. Y. Choi, J. Park, B. H. Lee, J. E. Yang, J. B. Park, S. O'Grady, D.-Y. Kim, P. D. Ryu, S.-W. Joo and S. Y. Lee, "Nuclear Localization and Functional Characteristics of Voltage-gated Potassium Channel Kv1.3," *The Journal of Biological Chemistry,* pp. 12547-12557, 15 May 2015.

[42] J.-H. Lee, J.-W. Park, J. K. Byun, H. K. Kim, P. D. Ryu, S. Y. Lee and D.-Y. Kim, "Silencing of voltage-gated potassium channel Kv9.3 inhibits proliferation in human colon and lung carcinoma cells," *Oncotarget,* pp. 8132-8143, 10 March 2015.

[43] G. A. Gutman, G. Chandy, S. Grissmer, M. Lazdunski, D. McKinnon, L. A. Pardo, G. A. Robertson, B. Rudy, M. C. Sanguinetti, W. Stuhmer and X. Wang, "International Union of Pharmacology. LIII. Nomenclature and Molecular Relationships of Voltage-Gated Potassium Channels," *Pharmacological Reviews,* pp. 473-508, 2005.

[44] M. S. Song, S. M. Park, S. J. Park, J. H. Byun, H. J. Jin, S. H. Seo, P. D. Ryu and S. Y. Lee, "Kv3.1 and Kv3.4 are involved in cancer cell migration and invasion," *International Journal of Molecular Sciences,* pp. 1-17, 2 April 2018.

[45] A. Girault, A. Privé, N. T. N. Trinh, O. Bardou, F. Pasquale, P. Joubert, R. Bertrand and E. Brochiero, "Identification of KvLQT1 K+ channels as new regulators of non-small cell lung cancer cell proliferation and migration," *International Journal of Oncology,* pp. 838-848, 25 November 2014.

[46] S.-z. Chen, M. Jiang and Y.-s. Zhen, "HERG K+ channel expression-related chemosensitivity in cancer cells and its modulation by erythromycin," *Cancer Chemotherapy Pharmacology,* pp. 212-220, 6 April 2005.

[47] E. Bulk, A.-S. Ay, M. Hammadi, H. Ouadid-Ahidouch, S. Schelhaas, A. Hascher, C. Rohde, N. H. Thoennissen, R. Wiewrodt, E. Schmidt, A. Marra, L. Hillejan, A. H. Jacobs and H.-U. Klein, "Epigenetic dysregulation of Kca3.1 channels induces poor prognosis in lung cancer," *International Journal of Cancer,* pp. 1306-1317, 2015.

[48] F. G. Ridge, M. Duszyk and A. S. French, "A large conductance, Ca2+-activated K+ channel in a human lung epithelial cell line (A549)," *Biochimica et Biophysica Acta,* pp. 249-258, 19 March 1997.

[49] S. Jovanovic, R. M. Crawford, H. J. Ranki and A. Jovanovic, "Large Conductance Ca2+-Activated K+ Channels Sense Acute Changes in Oxygen Tension in Alveolar Epithelial Cells," *Am J Respir Cell Mol Biol.,* pp. 363-372, 28 March 2003.

[50] H. K. Plummer, M. S. Dhar, M. Cekanova and H. M. Schuller, "Expression of G-protein inwardly rectifying potassium channels (GIRKs) in lung cancer cell lines," *BioMed Central,* 18 August 2005.

[51] K. Leithner, B. Hirschmugl, Y. Li, B. Tang, R. Rapp, C. Nagaraj, E. Stacher, P. Stiegler, J.

Lindenmann, A. Olschewski, H. Olschewski and A. Hrzenjak, "TASK-1 Regulates Apoptosis and Proliferation in a Subset of Non-Small Cell Lung Cancers," *PLOS ONE,* 13 June 2016.

[52] S. Roger, J. Rollin, A. Brascu, P. Besson, P.-I. Raynal, S. Iochmann, M. Lei, P. Bougnoux, Y. Gruel and J.-Y. Le Guennec, "Voltage-gated sodium channels potentiate the invasive capacities of human non-small-cell lung cancer cell lines," *The International Journal of Biochemistry & Cell Biology,* pp. 774-786, 20 January 2007.

[53] T. M. Campbell, M. J. Main and E. M. Fitzgerald, "Functional expression of the voltage-gated Na+-channel Nav1.7 is necessary for EGF-mediated invasion in human non-small cell lung cancer cells," *Journal of Cell Science,* pp. 4939-4949, 13 July 2013.

[54] A. Lazrak, A. Samanta and S. Matalon, "Biophysical properties and molecular characterization of amiloride-sensitive sodium channels in A549 cells," *American Journal of Physiology - Lung Cellular and Molecular Physiology,* pp. 848-857, 2000.

[55] P. J. Buchanan and K. D. McCloskey, "Cav channels and cancer: canonical functions indicate benefits of repurposed drugs as cancer therapeutics," *Eur Biophysics J,* pp. 621-633, 24 June 2016.

[56] M.-F. Hou, H.-C. Kuo, J.-H. Li, Y.-S. Wang, C.-C. Chang, K.-C. Chen, W.-C. Chen, C.-C. Chiu, S. Yang and W.-C. Chang, "Orai1/CRACM1 overexpression suppresses cell proliferation via attenuation of the store-operated calcium influx-mediated signalling pathway in A549 lung cancer cells," *Biochimica et Biophysica Acta,* pp. 1278-1284, 5 July 2011.

[57] L.-L. Yang, B.-C. Liu, X.-Y. Lu, Y. Yan, Y.-J. Zhai, B. Qing, P. W. Doetsch, X. Deng, T. L. Thai, A. A. Alli, C. E. Douglas, B.-Z. Shen and H.-P. Ma, "Inhibition of TRPC6 reduces non-small cell lung cancer cell proliferation and invasion," *Oncotarget,* pp. 5123-5134, 20 December 2017.

[58] X. Li, Q. Zhang, K. Fan, B. Li, H. Li, H. Qi, J. Guo, Y. Cao and H. Sun, "Overexpression of TRPV3 Correlates with Tumor Progression in Non-Small Cell Lung Cancer," *International Journal of Molecular Sciences,* pp. 1-13, 24 March 2016.

[59] P. Hou, R. Zhang, Y. Liu, J. Feng, W. Wang, Y. Wu and J. Ding, "Physiological Role of Kv1.3 Channel in T Lymphocyte Cell Investigated Quantitatively by Kinetic Modeling," *PLOS ONE,* 3 March 2014.

[60] J. R. Papreck, E. A. Martin, P. Lazzarini, D. Kang and D. Kim, "Modulation of K2p3.1 (TASK-1), K2p9.1 (TASK-3) and TASK-1/3 heteromer by reactive oxygen species," *Pflugers Arch.,* pp. 471-480, November 2012.

[61] A. Amcheslavsky, M. L. Wood, A. V. Yeromin, I. Parker, J. A. Freites, D. J. Tobias and M. D. Cahalan, "Molecular Biophysics of Orai Store-Operated Ca2+ Channels," *Biophysical Journal,* pp. 237-246, 26 November 2015.

[62] R. Grygorczyk, "Temperature dependence of Ca2+-activated K+ currents in the membrane of human erythrocytes," *Biochimica et Biophysica Acta,* pp. 159-168, 19 March 1987.

[63] R. Ranjan, M. Schartner and N. Khanna, "Channelpedia," 2005-2019. [Online]. Available: http://channelpedia.epfl.ch/ionchannels/3. [Accessed 15 01 2019].

[64] B. Fioretti, F. Franciolini and L. Catacuzzeno, "A model of intracellular Ca2+ oscillations based on the activity of the intermediate-conductance Ca2+-activated K+ channels," *Biophysical Chemistry,* pp. 17-23, 3 September 2004.

[65] A. Destexhe and J. R. Huguenard, "Nonlinear Thermodynamic Models of Voltage-Dependent Currents," *Journal of Computational Neuroscience 9,* pp. 259-270, 17 February 2000.

[66] M. Islam, Transient Receptor Potential Channels, Springer, 2011.

8. Appendix

Table 12 shows the alternative names of all in the thesis mentioned ion channels.

Common name	Alternative names
K_V1.1	KCNA1, EA1, MK1, AEMK, HBK1, HUK1, MBK1, RBK1, potassium voltage-gated channel subfamily A member 1
K_V1.2	KCNA2, HK4, MK2, HBK5, NGK1, RBK2, HUKIV, EIEE32, potassium voltage-gated channel subfamily A member 2
K_V1.3	KCNA3, MK3, HGK5, HLK3, PCN3, HPCN3, HUKIII, potassium voltage-gated channel subfamily A member 3
K_V1.5	KCNA5, HK2, HCK1, PCN1, ATFB7, HPCN1, potassium voltage-gated channel subfamily A member 5
K_V2.1	KCNB1, DRK1, potassium voltage-gated channel subfamily B member 1
K_V2.2	KCNB2, potassium voltage-gated channel subfamily B member 2
K_V3.1	KCNC1, KV4, EPM7, NGK2, potassium voltage-gated subfamily C member 1
K_V3.3	KCNC3, SCA13, KSHIIID, potassium voltage-gated channel subfamily C member 3
K_V3.4	KCNC4, C1orf30, KSHIIIC, HKSHIIIC, potassium voltage-gated channel subfamily C member 4
K_V7.1	KCNQ1, LQT, RWS, WRS, LQT1, SQT2, ATFB1, ATFB3, JLNS1, KCNA8, KCNA9, K_V1.9, KVLQT1, potassium voltage-gated channel subfamily Q member 1
K_V7.3	KCNQ3, EBN2, BFNC2, potassium voltage-gated channel subfamily Q member 3
K_V9.3	KCNS3, potassium voltage-gated channel modifier subfamily S member 3
K_V10.1	KCNH1, EAG, EAG1, ZLS1, TMBTS, h-eag, hEAG1, potassium voltage-gated channel subfamily H member 1
K_V11.1	KCNH2, ERG1, HERG, LQT2, SQT1, ERG-1, H-ERG, HERG1, potassium voltage-gated channel subfamily H member 2
K_{Ca}1.1	KCNMA1, SLO, BKTM, SLO1, hSlo, MaxiK, PNKD3, SAKCA, mSLO1, CADEDS, SLO-ALPHA, ba205K10.1, potassium calcium-activated channel subfamily M alpha 1
K_{Ca}2.1	KCNN1, SK1, hSK1, SKCA1, potassium calcium-activated channel subfamily N member 1
K_{Ca}2.2	KCNN2, SK2, hSK2, SKCA2, SKCa 2, potassium calcium-activated channel subfamily N member 2
K_{Ca}2.3	KCNN3, SK3, hSK3, SKCA3, potassium calcium-activated channel subfamily N member 3
K_{Ca}3.1	KCNN4, IK, IK1, SK4, DHS2, KCA4, hSK4, IKCA1, hKCa4, hIKCa1, potassium calcium-activated channel subfamily N member 4

$K_{Ca}4.2$	KCNT2, SLICK, EIEE57, SLO2.1, potassium sodium-activated channel subfamily T member 2
$K_{2P}1.1$	KCNK1, DPK, HOHO, K2P1, KCNO1, TWIK1, TWIK-1, potassium two pore domain channel subfamily K member 1
$K_{2p}2.1$	CNK2, TREK, TPKC1, TREK1, TREK-1, hTREK-1c, hTREK-1e, potassium two pore domain channel subfamily K member 2
$K_{2p}3.1$	KCNK3, OAT1, PPH4, TASK, TBAK1, TASK-1, potassium two pore domain channel subfamily K member 3
$K_{2p}5.1$	KCNK5, TASK2, KCNK5b, TASK-2, potassium two pore domain channel subfamily K member 5
$K_{2p}9.1$	KCNK9, KT3.2, TASK3, TASK-3, potassium two pore domain channel subfamily K member 9
$K_{ir}2.1$	KCNJ2, IRK1, LQT7, SQT3, ATFB9, HHIRK1, HHBIRK1, potassium voltage-gated channel subfamily J member 2
$K_{ir}3.1$	KCNJ3, KGA, GIRK1, potassium voltage-gated channel subfamily J member 3
$K_{ir}3.2$	KCNJ6, BIR1, GIRK2, KATP2, KCNJ7, KPLBS, GIRK-2, KATP-2, hiGIRK2, potassium voltage-gated channel subfamily J member 6
$K_{ir}3.3$	KCNJ9, GIRK3, potassium voltage-gated channel subfamily J member 9
$K_{ir}3.4$	KCNJ5, CIR, GIRK4, KATP1, LQT13, potassium voltage-gated channel subfamily J member 5
$K_V b1.3$	KCNAB1, hKvb3, AKR6A3, hKvBeta3, KV-BETA-1, potassium voltage-gated channel subfamily A member regulatory beta subunit 1
KCNAB2	AKR6A5, KCNA2B, HKvbeta2, KV-BETA-2, HKvbeta2.1, HKvbeta2.2, potassium voltage-gated channel subfamily A regulatory beta subunit 2
KCNMB4	potassium calcium-activated channel subfamily M regulatory beta subunit 4
$Na_V1.2$	SCN2A, HBA, NAC2, BFIC3, BFIS3, BFNIS, HBSCI, EIEE11, HBSCII, SCN2A1, SCN2A2, sodium voltage-gated channel alpha subunit 2
$Na_V1.4$	SCN4A, HYPP, SkM1, CMS16, HYKPP, NAC1A, HOKPP2, sodium voltage-gated channel alpha subunit 4
$Na_V1.5$	SCN5A, HB1, HB2, HH1, IVF, VF1, HBBD, ICCD, LQT3, SSS1, CDCD2, CMD1E, CMPD2, PFHB1, sodium voltage-gated channel alpha subunit 5
$Na_V1.7$	SCN9A, PN1, ETHA, NENA, SFNP, FEB3B, NE-NA, GEFSP7, HSAN2D, sodium voltage-gated channel alpha subunit 9
$Na_V2.1$, $Na_V2.2$	SCN7A, NaG, SCN6A, sodium voltage-gated channel alpha subunit 7
ASIC1	ASIC, ACCN2, BNaC2, acid sensing ion channel subunit 1
ASIC2	ACCN, BNC1, MDEG, ACCN1, BNaC1, ASIC2a, hBNaC1, acid sensing ion channel subunit 2
ASIC3	ACCN3, TNAC1, DRASIC, SLNAC1, acid sensing ion channel subunit 3
ENaC	SCNN1A, BESC2, ENaCa, SCNEA, SCNN1, LIDLS3, ENACalpha, sodium channel epithelial 1 alpha subunit
SCN4B	LQT10, ATFB17, Navbeta4, sodium voltage-gated channel beta

	subunit 4
SCNN1B	BESC1, ENaCb, SCNEB, LIDLS1, ENaCbeta, sodium channel epithelial 1 beta subunit
SCNN1G	PHA1, BESC3, ENaCg, LDLS2, SCNEG, ENaCgamma, sodium channel epithelial 1 gamma subunit
$Ca_V1.1$	CACNA1S, MHS5, HOKPP, TTPP1, HOKPP1, hypoPP, CCHL1A3, CACNL1A3, calcium voltage-gated channel subunit alpha1 S
$Ca_V1.2$	CACNA1C, TS, LQT8, CACH2, CACN2, CCHL1A1, CACNL1A1, calcium voltage-gated channel subunit alpha1 C
$Ca_V1.3$	CACNA1D, CACH3, CACN4, PASNA, SANDD, CCHL1A2, CACNL1A2, calcium voltage-gated channel subunit alpha1 D
$Ca_v1.4$	CACNA1F, JM8, OA2, AIED, COD3, COD4, JMC8, CORDX, CSNB2, CORDX3, CSNB2A, CSNBX2, Cav1.4alpha1, calcium voltage-gated channel subunit alpha 1 F
$Ca_V2.3$	CACNA1E, BII, CACH6, gm139, EIEE69, CACNL1A6, calcium voltage-gated channel subunit alpha1 E
$Ca_V3.1$	CACNA1G, NBR13, SCA42, SCA42ND, Ca(V)T.1, calcium voltage-gated channel subunit alpha1 G
$Ca_V3.2$	CACNA1H, ECA6, EIG6, HALD4, CACNA1HB, calcium voltage-gated channel subunit alpha1 H
$Ca_V3.3$	CACNA1I, calcium voltage-gated channel subunit alpha1 I
ORAI1	IMD9, TAM2, ORAT1, CRACM1, TMEM142A, calcium release-activated calcium modulator 1
CLCC1	MCLC, chloride channel CLIC like 1
CLCN3	CLC3, CIC-3, chloride voltage-gated channel 3
CLCN7	CLC7, CLC-7, OPTA2, OPTB4, PPP1R63, chloride voltage-gated channel 7
CLIC6	CLIC1L, chloride intracellular channel 6
CLIC3	chloride intracellular channel 3
CLIC4	H1, huH1, p64H1, CLIC4L, MTCLIC, chloride intracellular channel 4
CLIC5	MST130, DFNB102, DFNB103, MSTP130, chloride intracellular channel 5
ANO1	DOG1, TAOS2, ORAOV2, TMEM16A, anoctamin 1
TRPC1	TRP1, HTRP-1, transient receptor potential cation channel subfamily C member 1
TRPC3	TRP3, SCA41, transient receptor potential cation channel subfamily C member 3
TRPC4	TRP4, HTRP4, HTRP-4, transient receptor potential cation channel subfamily C member 4
TRPC6	TRP6, FSGS2, transient receptor potential cation channel subfamily C member 6
TRPV1	VR1, transient receptor potential cation channel subfamily V member 1
TRPV2	VRL, VRL1, VRL-1, transient receptor potential cation channel subfamily V member 2
TRPV3	OLMS, VRL3, FNEPPK2, transient receptor potential cation channel

	subfamily V member 3
TRPV5	CAT2, ECAC1, OTRPC3, transient receptor potential cation channel subfamily V member 5
TRPV6	CAT1, CATL, ZFAB, ECAC2, ABP/ZF, HRPTTN, LP6728, HSA277909, transient receptor potential cation channel subfamily V member 6
TRPM2	KNP3, EREG1, TRPC7, LTRPC2, NUDT9H, LTrpC-2, NUDT9L1, transient receptor potential cation channel subfamily M member 2
TRPM7	CHAK, CHAK1, ALSPDC, LTRPC7, LTrpC-7, TRP-PLIK, transient receptor potential cation channel subfamily M member 7
TRPM8	TRPP8, LTRPC6, trp-p8, LTrpC-6, transient receptor potential cation channel subfamily M member 8
CHRNA7	NACHRA7, CHRNA7-2, cholinergic receptor nicotinic alpha 7 subunit

TABLE 12: Alternative names of all mentioned ion channels